



**HAL**  
open science

## Not so local: the population genetics of convergent adaptation in maize and teosinte

Silas Tittes, Anne Lorant, Sean Mcginty, James Holland, Jose de Jesus Sánchez-González, Arun Seetharam, Maud Tenailon, Jeffrey Ross-Ibarra

### ► To cite this version:

Silas Tittes, Anne Lorant, Sean Mcginty, James Holland, Jose de Jesus Sánchez-González, et al.. Not so local: the population genetics of convergent adaptation in maize and teosinte. 2023. hal-04291074

**HAL Id: hal-04291074**

**<https://hal.science/hal-04291074>**

Preprint submitted on 17 Nov 2023

**HAL** is a multi-disciplinary open access archive for the deposit and dissemination of scientific research documents, whether they are published or not. The documents may come from teaching and research institutions in France or abroad, or from public or private research centers.

L'archive ouverte pluridisciplinaire **HAL**, est destinée au dépôt et à la diffusion de documents scientifiques de niveau recherche, publiés ou non, émanant des établissements d'enseignement et de recherche français ou étrangers, des laboratoires publics ou privés.



# Not so local: the population genetics of convergent adaptation in maize and teosinte.

Silas Tittes<sup>a,b,c,1</sup>, Anne Lorant<sup>d</sup>, Sean McGinty<sup>e</sup>, James B. Holland<sup>f</sup>, Jose de Jesus Sánchez-González<sup>g</sup>, Arun Seetharam<sup>h</sup>, Maud Tenaillon<sup>i</sup> and Jeffrey Ross-Ibarra<sup>b,c,j,1</sup>

<sup>a</sup>Institute of Ecology and Evolution, University of Oregon, Eugene, OR 97403, USA, <sup>b</sup>Dept. of Evolution and Ecology, University of California, Davis, CA 95616, USA, <sup>c</sup>Center for Population Biology, University of California, Davis, CA 95616, USA, <sup>d</sup>Department of Plant Sciences, University of California, Davis, CA 95616, USA, <sup>e</sup>Dept. of Integrative Genetics and Genomics, University of California, Davis, CA 95616, USA, <sup>f</sup>United States Department of Agriculture – Agriculture Research Service, Raleigh, NC 27695 USA and Department of Crop and Soil Sciences, North Carolina State University, <sup>g</sup>Centro Universitario de Ciencias Biológicas y Agropecuarias, Universidad de Guadalajara, Zapopan, Jalisco CP45110, México, <sup>h</sup>Department of Ecology, Evolution, and Organismal Biology; Genome Informatics Facility, Iowa State University, Ames, IA 50011, USA, <sup>i</sup>Génétique Quantitative et Evolution - Le Moulon, Université Paris-Saclay, INRAE, CNRS, AgroParisTech, 91190, Gif-sur-Yvette, France, <sup>j</sup>Genome Center, University of California, Davis, CA 95616, USA

## ABSTRACT

What is the genetic architecture of local adaptation and what is the geographic scale over which it operates? We investigated patterns of local and convergent adaptation in five sympatric population pairs of traditionally cultivated maize and its wild relative teosinte (*Zea mays* subsp. *parviglumis*). We found that signatures of local adaptation based on the inference of adaptive fixations and selective sweeps are frequently exclusive to individual populations, more so in teosinte compared to maize. However, for both maize and teosinte, selective sweeps are also frequently shared by several populations, and often between subspecies. We were further able to infer that selective sweeps were shared among populations most often via migration, though sharing via standing variation was also common. Our analyses suggest that teosinte has been a continued source of beneficial alleles for maize, even after domestication, and that maize populations have facilitated adaptation in teosinte by moving beneficial alleles across the landscape. Taken together, our results suggest local adaptation in maize and teosinte has an intermediate geographic scale, one that is larger than individual populations, but smaller than the species range.

**KEYWORDS** Local Adaptation, Convergent Adaptation, Maize, Teosinte

1

## 2 Introduction

3 As populations diverge and occupy new regions, they become  
4 locally adapted to the novel ecological conditions that they en-  
5 counter. Decades of empirical work have carefully documented  
6 evidence for local adaptation, including the use of common  
7 garden and reciprocal transplant studies demonstrating that  
8 populations express higher fitness in their home environment  
9 (Clausen *et al.* 1948) as well as quantitative genetic approaches  
10 that show selection has acted on individual traits to make or-  
11 ganisms better suited to their ecological conditions (Savolainen  
12 *et al.* 2013). It is clear from these studies that local adaptation is  
13 pervasive in natural populations.

14 One important but understudied aspect of local adaptation is  
15 its geographic scale. Empirical studies have documented adap-  
16 tation at multiple scales, from microgeographic differentiation  
17 among mesic and xeric habitats along a single hillside (Ham-  
18 rick and Allard 1972) to regional (Lowry *et al.* 2008; Whitehead  
19 *et al.* 2011) and even global scales (Colosimo *et al.* 2005). A key  
20 factor determining the geographic scale of local adaptation is  
21 the distribution of the biotic and abiotic challenges to which  
22 organisms are adapting, as these features place limits on the

23 locations over which an allele remains beneficial. Environmental  
24 features overlap with each other to varying degrees (Tuanmu  
25 and Jetz 2015). The degree of overlap between environmen-  
26 tal features may be important if mutations are pleiotropic, as  
27 an allele may not be beneficial when integrating its effect over  
28 multiple selective pressures (Chevin *et al.* 2010).

29 The geographic scale of local adaptation depends, too, on  
30 population structure. Gossmann *et al.* (2010) showed that the  
31 estimates of the proportion of new mutations fixed by natural  
32 selection across a number of plant species tended to overlap  
33 with zero, suggesting there is little evidence for adaptation at  
34 non-synonymous sites (though see Williamson *et al.* 2014; Geist  
35 *et al.* 2019 for more recent non-zero estimates of  $\alpha$  in two plant  
36 taxa). One potential explanation raised by the authors for this  
37 surprising finding was that natural populations are often struc-  
38 tured, such that very few adaptations would be expected to  
39 be common over the entire range of the species' distribution.  
40 Indeed, even when selective pressures are shared across popula-  
41 tions, structure can hinder a species' adaptation by limiting the  
42 spread of beneficial alleles across its range (Bourne *et al.* 2014).  
43 Consistent with this, Fournier-Level *et al.* (2011) conducted a  
44 continent-scale survey across strongly structured populations  
45 of *Arabidopsis thaliana*, finding that alleles which increase fitness  
46 tended to occur over a restricted geographic scale. But it remains  
47 unclear if the scales identified in *Arabidopsis* are common to lo-

<sup>1</sup> For correspondence, Dept. of Evolution and Ecology, University of California, Davis, CA, USA E-mail: stittes@ucdavis.edu; rossibarra@ucdavis.edu



cal adaptation across the entire genome, and how similar the general patterns are across taxa.

The majority of local adaptation studies are motivated by conspicuous differences in the phenotypes or environments of two or more populations. As such, many instances of local adaptation that are occurring, as well as the underlying beneficial mutations being selected, may go overlooked. This hinders our ability to draw more general conclusions about the overall frequency and impact of local adaptation on a given population's evolutionary history.

Using population genetic approaches, we can compare the observed distribution of beneficial alleles across multiple populations to get a more holistic description of the history of selection. The patterns of selective sweeps and adaptive fixations that are exclusive to or shared among multiple populations can be used to measure a beneficial allele's geographic extent, which is influenced by the factors outlined above. If we infer multiple structured populations have fixed the same beneficial allele, this suggests that pleiotropy has not disrupted the adaptive value of the allele across environments or that the populations share a sufficiently similar set of selective pressures. Assessment of the relative frequency and geographic extent of unique and shared beneficial alleles thus allows us to quantify the scale of local adaptation. Additionally, when multiple populations do share an adaptive allele, we can infer the mode by which sharing occurred (Lee and Coop 2017), providing further insights about the environmental and genetic context of each adaptation as well as the processes underlying allele sharing among populations.

Motivated to improve our understanding about the genetic basis of local adaptation and its geographic scale, we set out to use population genetic approaches to understand patterns of adaptation via selective sweeps in multiple discrete populations of domesticated maize *Zea mays* ssp. *mays* and its wild relative teosinte *Zea mays* ssp. *parviglumis* growing across their native range in Mexico. *Zea mays* is an annual grass, native to southern Mexico. Maize was domesticated  $\approx 9,000$  years ago (Piperno et al. 2009) from its common ancestor with the extant annual grass teosinte, but traditional open-pollinated populations maintain an extremely large population size and a surprising amount of diversity (Bellon et al. 2018). Maize is also the world's most productive crop (Ranum et al. 2014), and an important model system for genetics (Nannas and Dawe 2015).

Previous work in both maize and teosinte has demonstrated clear population structure at both regional (Pyhäjärvi et al. 2013) and fine (Van Heerwaarden et al. 2010; Hufford et al. 2011) scales, and population genetic and common garden studies in both subspecies have shown clear signatures of populations being adapted to ecological conditions across their native range (Janzen et al. 2021). In maize this includes local adaptation to high elevation (Fustier et al. 2019; Gates et al. 2019), phosphorous (Rodriguez-Zapata et al. 2021), temperature (Butler and Huybers 2013), and day length (Swarts et al. 2017). Similarly, studies of teosinte have documented local adaptation based on features such as the differential patterns of microbial community recruitment (O'Brien et al. 2019), elevation (Fustier et al. 2019, 2017), and temperature and phosphorous (Aguirre-Liguori et al. 2019).

Studying local adaptation of maize and teosinte across the same geographic locations presents opportunities to disentangle multiple processes that interact with adaptation. For example, the effect of the domestication process in maize populations and their ongoing interaction and dependence on humans has created changes in the timing and types of selection imposed across

all populations, as well as changes in demography (Wright et al. 2005). Based on population structure and differences in the abiotic environment among populations, we anticipated that local adaptation would have a small geographic scale. We predicted that sweeps would be exclusive to individual populations, and that adaptations shared between subspecies would be limited to sympatric pairs of populations growing in similar environments and with ample opportunity for genetic exchange. Because of domestication and the ongoing migration facilitated by humans, we expected that maize would show more shared adaptations, leading to a relatively larger geographic scale of local adaptation. Contrary to our predictions, our results suggest adaptations are often shared across two or more populations, and commonly between maize and teosinte. We also found that migration and standing variation have played an important role as sources of beneficial alleles, including many that are shared across the two subspecies.

## Results

We sampled teosinte (*Zea mays* subsp. *parviglumis*) individuals from six locations across its native range, along with a nearby (sympatric) population of traditionally cultivated open-pollinated maize (commonly referred to as landraces) at five of these locations (Figure 1C). We sampled ten individuals from each population for each subspecies, with the exception of the Palmar Chico populations, where we took advantage of 55 and 50 individuals previously sampled for maize and teosinte, respectively (Table S1, Supplement I, Chen et al. 2020). In most cases, results for both Palmar Chico populations were down-sampled to ten randomly selected individuals to facilitate comparisons to the other populations. We did, however, use a second random sample of the Palmar Chico populations to estimate the precision of our inference of selective sweeps (see below in Results and Methods).

Rangewide samples for each subspecies were constructed by randomly selecting one individual from each population. All 195 individuals were sequenced at 20 to 25x coverage and aligned to version 5 of the *Zea mays* B73 reference genome (Hufford et al. 2021; Portwood et al. 2019). Analyses were based on genotype likelihoods (Korneliussen et al. 2014) except in cases where called genotypes were required (see Methods).

### **Subspecies and populations are genetically distinct despite evidence of gene flow.**

To assess the relationships among our sampled populations, we constructed a population-level phylogeny using Treemix (Pickrell and Pritchard 2012 v.1.13). As anticipated from previous work (Buckler and Holtsford 1996; Hufford et al. 2012), we found clear divergence between two clades composed of maize and teosinte populations, though the relationship among geographic locations differed between the subspecies (Figure 1B).

Within subspecies, populations were genetically distinct from one another. Using NGSadmixture (Skotte et al. 2013), there was little evidence of admixture between populations of the same subspecies; only two of the sampled individuals revealed evidence of mixed ancestry (Figure 1A and 1D).

Despite the clear phylogenetic separation between the two subspecies, there is evidence for gene flow between maize and teosinte populations. We conducted f4 tests using Treemix (Pickrell and Pritchard 2012), and found that all populations showed some evidence of gene flow with various populations of the other subspecies, as measured by the high absolute Z-Scores of



170 the  $f_4$  statistic. Overall, we found little evidence of increased  
 171 gene flow between sympatric pairs (Figure 1E), but Z-scores  
 172 were sensitive to the specific combinations of non-focal popu-  
 173 lations included in each test (Table S2). Specifically, we found  
 174 that elevated  $f_4$  tests almost always included the maize popu-  
 175 lation from Crucero Lagunitas ( $p < 2 \times 10^{-10}$ ), which was true  
 176 whether or not the  $f_4$  test included its sympatric teosinte.

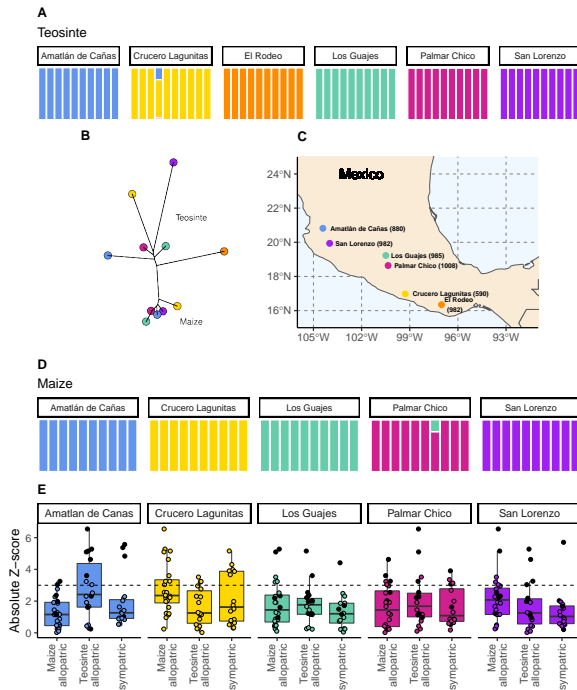


**Figure 1 | The geographic distribution, population structure, and gene flow of maize and teosinte populations.** (A and D) Admixture proportions among populations within subspecies. The dominant cluster in each population is colored by sampling location. (B) The unrooted tree of maize and teosinte populations. (C) Geographic sampling locations for the studied maize and teosinte populations. (E)  $F_4$  tests to quantify evidence of gene flow between the subspecies for allopatric and sympatric population pairs. Each point in (E) reports the absolute Z-Score for an  $f_4$  test, where a given focal population was partnered with another population of the same subspecies as a sister node, and two other populations from the other subspecies as a sister clade (see Methods for further details). Black points show  $f_4$  tests that included maize from Crucero Lagunitas, otherwise points are colored by focal population. The dotted line corresponds to our chosen significance threshold ( $p = 0.001$ ).

**Populations vary in their diversity, demography, and history of inbreeding**

We estimated pairwise nucleotide diversity ( $\pi$ ) and Tajima's D in non-overlapping 100Kb windows along the genome in our sampled populations using ANGSD (Korneliussen et al. 2014). For all populations,  $\pi$  was in the range of 0.006 to 0.01, consistent

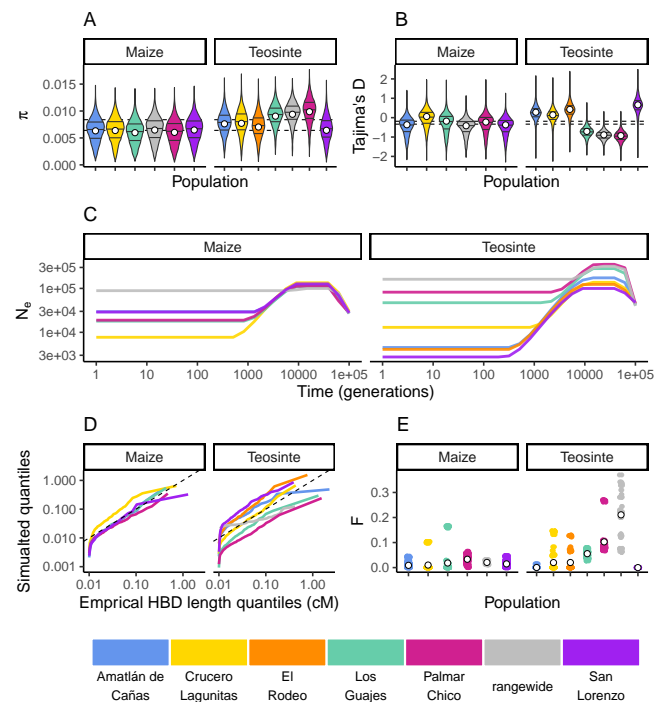


**Figure 2 | Inbreeding, diversity, and demography.** The distribution of  $\pi$  (A) and Tajima's D (B) calculated in 100Kb windows for maize and teosinte populations. Dashed lines show the median values for the two subspecies. Filled white points show the median values of each statistic generated from coalescent simulations under the demographic history inferred for each population. Colors for each population are as in Figure 1 and are shown at the bottom of the figure. (C) The inferred demography for each population. (D) The quantile of observed Homozygosity By Descent (HBD) lengths (cM) versus those simulated under each population demography. Dashed lines shows the 1:1 correspondence between the axes. (E) The distribution of inbreeding coefficients in each population. Filled white points are the average values for each population.

with both previous Sanger (Wright et al. 2005) and short-read (Hufford et al. 2012) estimates for both subspecies. Variation in Tajima's D and  $\pi$  was greater among populations of teosinte than maize (Figures 2 A and B, Table S2).

We independently estimated the demographic history for each population from their respective site frequency spectra using mushi (DeWitt et al. 2021 v0.2.0). All histories estimated a bottleneck that started approximately 10 thousand generations ago (assuming a mutation rate of  $3 \times 10^{-8}$  (Clark et al. 2005) (Figure 2E).

Teosinte is a primarily outcrossing grass (Hufford 2010), and regional maize farming practices promote outcrossing as well (Bellon et al. 2018). To validate our estimated demography and characterize the history of inbreeding in each population, we compared the empirical quantiles of homozygosity by descent (HBD) segments inferred using IBDseq (Browning and Browning 2013) to those simulated under the demography of each population. With the exception of the smallest HBD segments, which are more prone to inaccurate estimation, the simulated



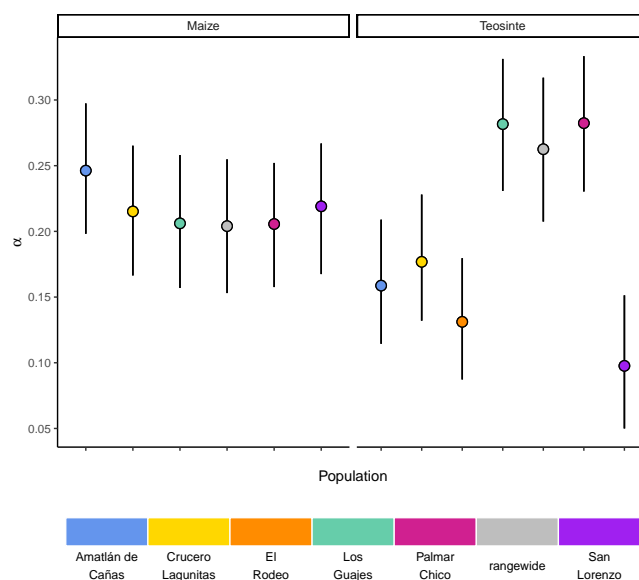
204 quantiles generally resemble the empirical quantiles (Figure 2D).  
 205 This indicates that the inbreeding history of our population is  
 206 adequately captured by the demography. However, consistent  
 207 with previous studies of teosinte (Hufford 2010), we do see  
 208 variation in the distributions of HDB among populations. For  
 209 example, the size distribution of HDB segments in San Lorenzo  
 210 and Los Guajes were consistently larger than those simulated  
 211 from their demographies, particularly for the smallest segments.  
 212 This likely reflects inbreeding caused by demographic changes,  
 213 particularly those further in the past that may not be not as  
 214 accurately captured by our demography inferences. These re-  
 215 sults are consistent with previous studies that found evidence  
 216 for historical inbreeding in teosinte, particularly in individuals  
 217 sampled from San Lorenzo (Pyhäjärvi et al. 2013). Lastly, we esti-  
 218 mated inbreeding coefficients (F) using ngsRelate (Hanghøj et al.  
 219 2019). Although inbreeding coefficients were as high as 0.37, the  
 220 mean value of F was  $0.017 \pm 0.001$  (SE) and  $0.033 \pm 0.001$  (SE)  
 221 for maize and teosinte (respectively), (Figure 2E). These values  
 222 are consistent with prior estimates of the rate of outcrossing of  
 223  $\approx 3\%$  in teosinte (Hufford et al. 2011) and suggest there has been  
 224 relatively little inbreeding in either subspecies in the recent past.

225 **Rangewide estimates of the proportion of mutations fixed by**  
 226 **natural selection ( $\alpha$ ) are commensurate with that of individual**  
 227 **populations**

228 If populations are relatively isolated and adaptation occurs pri-  
 229 marily via local selective sweeps, then we expect that most  
 230 adaptive fixations will happen locally in individual populations  
 231 rather than across the entire species range. This pattern should  
 232 become even stronger if alleles experience negative pleiotropy,  
 233 such that they are only adaptive in one environment and deleteri-  
 234 ous in others, further inhibiting the ability of such alleles to fix  
 235 rangewide. If adaptation via sweeps is commonly restricted to  
 236 individual populations, using a broad geographic sample to rep-  
 237 resent a population could underestimate the number of adaptive  
 238 substitutions that occur (Gossmann et al. 2010). To test this, we esti-  
 239 mated the proportion of mutations fixed by adaptive evolution  
 240 ( $\alpha$ ) (Smith and Eyre-Walker 2002) across all of our populations  
 241 and the rangewide samples for both subspecies. We estimated  
 242  $\alpha$  jointly among all populations by fitting a non-linear mixed-  
 243 effect model based on the asymptotic McDonald-Kreitman test  
 244 (Messer and Petrov 2013). Across populations,  $\alpha$  varied between  
 245 0.097 (teosinte San Lorenzo) and 0.282 (teosinte Palmar Chico),  
 246 with more variation among teosinte populations (Figure 3). In  
 247 contrast to our expectations, rangewide estimates of  $\alpha$  were com-  
 248 mensurate with individual populations. We additionally evalu-  
 249 ated estimates of  $\alpha$  for specific mutation types, which has been  
 250 shown to be lower at sites mutating from A/T to G/C, due to  
 251 the effects of GC-biased gene conversion in *Arabidopsis* (Hämälä  
 252 and Tiffin 2020). While we do find some evidence that  $\alpha$  predic-  
 253 tions varied by mutation type (see Figure S2, Supplement III),  
 254 the patterns are the opposite of that found in *Arabidopsis*, per-  
 255 haps because of the increased level of methylation in maize and  
 256 the higher mutation rate at methylated cytosines. Even after  
 257 accounting for differences among mutation types, rangewide  
 258 values remained commensurate with that of the populations.

260 **Teosinte populations have a higher proportion of private**  
 261 **sweeps**

262 Our inferences of  $\alpha$  are based on substitutions at non-  
 263 synonymous sites. The functional space for selection to act



264 **Figure 3 The proportion of mutations fixed by natural selection.**  
 265 Estimated values of the proportion of mutations fixed by  
 266 natural selection ( $\alpha$ ) by population. Vertical lines show the 95%  
 267 credible interval.

268 on occurs over many other parts of the genome besides protein  
 269 coding bases, especially for large repetitive plant genomes (Mei  
 270 et al. 2018). To identify signatures of adaptation occurring any-  
 271 where in the genome, we used RAI<sub>SD</sub> (Alachiotis and Pavlidis  
 272 2018) to identify putative selective sweeps in each population,  
 273 where sweep regions were identified by merging  $\mu$  summary  
 274 statistic outliers using a threshold defined by coalescent simu-  
 275 lations under each population's estimated demography (see  
 276 Methods). Simulations suggest this approach has high accuracy  
 277 and power compared to alternative methods over a broad range  
 278 of scenarios (Alachiotis and Pavlidis 2018). To further assess  
 279 the precision of our sweep inferences, we compared the over-  
 280 lap in sweep regions from a second random sample from both  
 281 maize and teosinte from Palmar Chico. After optimizing over a  
 282 grid of hyperparameters for RAI<sub>SD</sub> (see Methods), we esti-  
 283 mated the proportion of sweeps shared between replicates to be 0.67  
 284 and 0.80 for maize and teosinte, respectively. This proportion  
 285 is consistent with the false positive rates for strongly selected  
 286 hard sweeps estimated from simulations under the demographic  
 287 histories (See Supplement IV). As such, a non-trivial number  
 288 of the putative sweep regions we inferred with RAI<sub>SD</sub> in other  
 289 populations are likely also false positives, though far fewer than  
 290 previously reported using alternative methods for identifying  
 291 sweep regions (Tittes et al. 2021).

292 We used the inferred sweep regions to assess the degree to  
 293 which adaptation is shared or locally restricted using the sweep  
 294 regions we identified. We determined how many sweep re-  
 295 gions were exclusive to one population (private), along with  
 296 the number of overlapping sweep regions shared across two  
 297 or more populations within and between the two subspecies.  
 298 Overall, sharing was common, though fewer sweeps were exclu-  
 299 sively shared between teosinte populations (Figure 4A). Across  
 300 teosinte populations, 22% of sweeps were private, which was  
 301 significantly greater than the 14% found in maize (binomial glm,  
 302  $p = 0.0026$ ; Figure 4B).



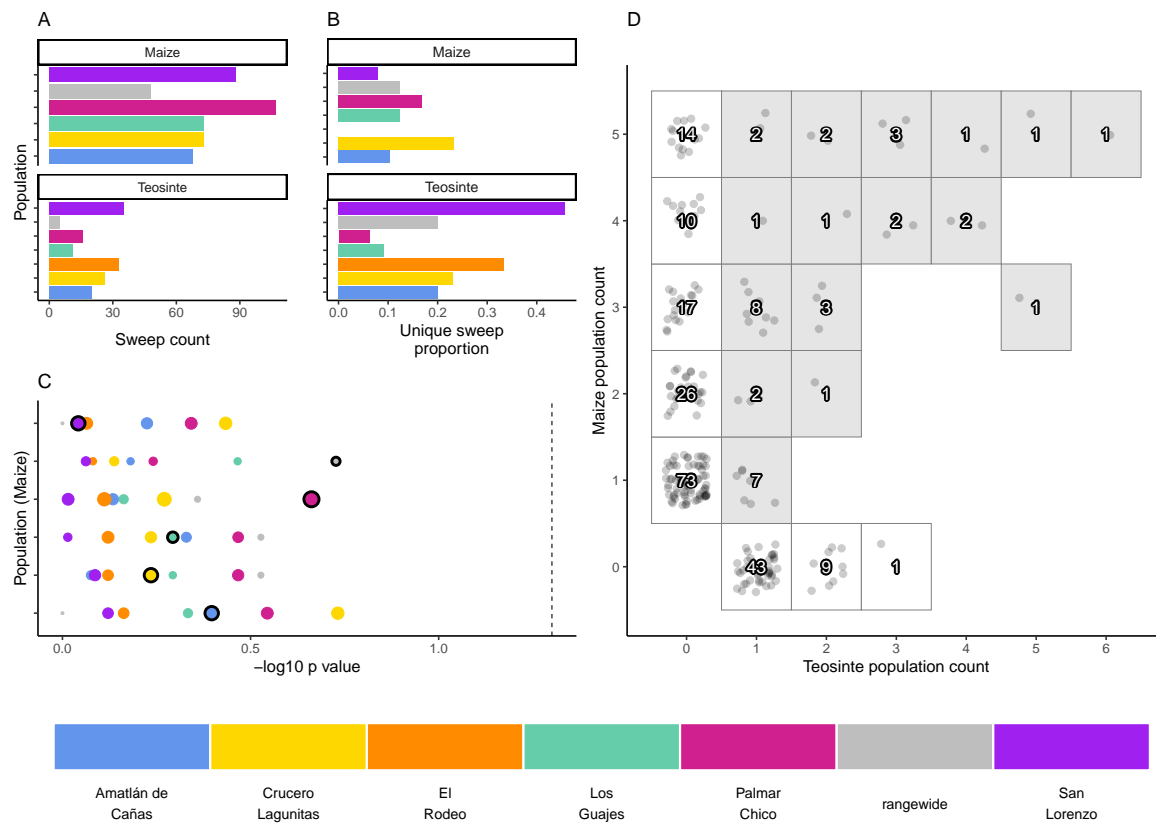


**Figure 4** The distribution of shared and private selective sweeps. (A) The total number of sweeps inferred in each population. (B) The proportion of sweeps that are unique to each population. (C) The negative log<sub>10</sub> p values for hypergeometric tests to identify maize-teosinte population pairs that shared more sweeps than expected by chance (see Methods). P values were adjusted for multiple tests using the Benjamini and Yekutieli method. Populations along the y axis are maize (order matches the legend below, with Amatlán de Cañas at the bottom), while the point color designates the teosinte population each maize population was paired with. Points with black outline highlight the sympatric population comparisons. Point size is scaled by the number of shared sweeps identified in each pair. The dotted line indicates our chosen significance level ( $p = 0.05$ ). (D) Counts of shared and unique sweeps broken down by how many maize and teosinte populations they occurred in. Grey boxes show sweeps shared across the two subspecies.

299 **Sympatric population pairs do not share more sweeps**

300 If local adaptation favors certain alleles in a given environment,  
 301 we might expect to see increased sharing of sweeps between  
 302 sympatric populations of maize and teosinte. To look for evi-  
 303 dence of such sharing, we used a hypergeometric test based on  
 304 the number of sweeps in each population and the number of  
 305 shared sweeps between population pairs, which allowed us to  
 306 test if sympatric population pairs tended to have more sharing  
 307 than expected by chance. In conducting this test, we incorpo-  
 308 rated our estimate of sweep precision (see Methods). Sympatric  
 309 pairs did not tend to have a lower p value than allopatric pairs,  
 310 and no population pair showed more sharing than expected  
 311 by chance (Figure 4). We additionally found that, despite evi-  
 312 dence that sweeps are commonly shared between maize and  
 313 teosinte (Figure 4D), there were zero sweeps exclusive to sym-  
 314 patric pairs; sweeps that were shared between sympatric pairs  
 315 always included at least one other allopatric population.

316 **Convergent adaptation from migration is common among**  
 317 **maize and teosinte populations**

318 In instances when two or more populations shared a sweep re-  
 319 gion, we used rdmC (Lee and Coop 2017; Tittes 2020) to infer the  
 320 most likely mode of convergence. We classified sweeps based on  
 321 which composite log-likelihood model was greatest out of four  
 322 possible models of convergence (independent mutations, migra-  
 323 tion, neutral, and standing variation). Of the 102 sweeps that  
 324 were shared by two or more populations, there were 1, 38, and  
 325 23 sweeps inferred to be convergent via independent mutations,  
 326 migration, or standing variation; and an additional 40 sweeps  
 327 inferred to be neutral (Figure 5C). The high proportion (37%) of  
 328 neutral models inferred by rdmC is consistent with our estimate  
 329 of sweep precision. We have higher confidence, however, that  
 330 regions inferred to be non-neutral with both RAiSD and rdmC  
 331 represent bona fide sweeps. The strength of support (measured  
 332 as the composite likelihood score of the best model relative to the  
 333 next best) varied among sweeps and modes of convergence, but  
 334 in general a single model tended to be clearly favored among  
 335 the alternatives (Figure 5A). Selection coefficients for sweeps



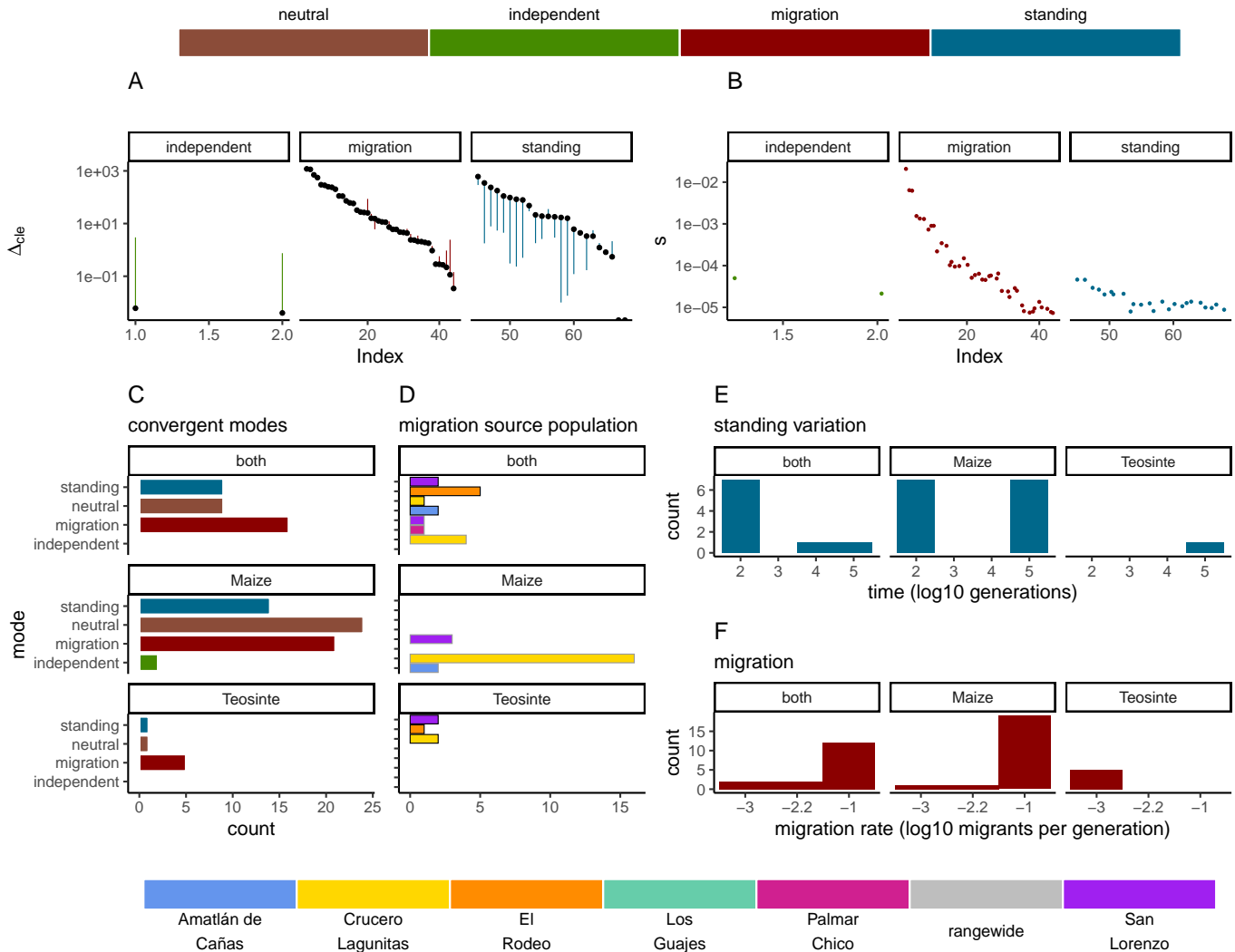


**Figure 5** Modes of convergent adaptation and affiliated parameters for shared selective sweeps. (A) The difference in composite likelihood scores for the best supported mode of convergent adaptation (colors in top legend) compared to next best mode (black points), and best mode compared to the neutral model (other end of each line segment above or below black point). (B) Selection coefficients colored by the most likely mode of convergent adaptation. (C) Number of shared sweeps for both subspecies that were inferred to be from each convergent adaptation mode. (D) The most likely source population for shared sweeps that converged via migration. Bars are colored by population (bottom legend) and are outlined in black for teosinte and grey for maize. (E) Observed frequency of the inferred time in generations that each selected allele persisted prior to selection for models of convergent adaptation via standing variation. (F) Observed frequency of each inferred migration rate value for models of convergent adaptation via migration. Panels C, D, E and F are partitioned by which subspecies shared the sweep.

336 varied among modes, with convergence via migration having  
 337 the highest average estimate (Figure 5B). When migration was  
 338 the mode of convergence and sweeps were shared by both  
 339 subspecies, teosinte El rodeo, and maize from Crucero Lagunitas  
 340 (Figure 5D). In convergence models with migration, we tested  
 341 migration rates between  $10^{-3}$  and  $10^{-1}$ . The most likely migra-  
 342 tion rate varied across sweeps, but tended to be  $10^{-1}$  for the  
 343 majority of sweeps shared by the two subspecies and sweeps  
 344 exclusive to maize. In contrast, the lowest migration rate ( $10^{-3}$ )  
 345 was always the most likely for sweeps exclusive to teosinte (Fig-  
 346

347 ure 5F). Together, these findings indicate that many alleles are  
 348 adaptive in the genomic background of both maize and teosinte,  
 349 and that adaptive alleles are commonly shared between the two  
 350 subspecies.

## 351 Discussion

### 352 Local adaptation occurs at intermediate scales

353 Gossmann *et al.* (2010) hypothesized that population structure  
 354 within a species could limit the fixation of adaptive alleles across  
 355 a species range, causing a reduction in the proportion of muta-



tions fixed by positive selection ( $\alpha$ ). Based on this hypothesis and the strong population structure we observed (Figure 1), we expected that rangewide samples would have smaller estimates of  $\alpha$ . Instead,  $\alpha$  for the rangewide samples of both maize and teosinte were commensurate with that of individual populations (Figure 3), a pattern that persisted even when we considered  $\alpha$  estimated from several different mutation types (Figure S2). This is inconsistent with the patterns we would expect fine-scale local adaptation to generate, where adaptive substitutions for a given population should not be shared by other populations experiencing their own distinct local selective pressures and antagonistic pleiotropy suppresses rangewide fixation in alternative environments. Our findings makes sense in the light of other work studying pleiotropy's impact on adaptive evolution in *Arabidopsis*, which found that most mutations impact few traits and that the genetic architecture was largely non-overlapping when studied across multiple environments (Frachon *et al.* 2017). Our results are consistent with models in which locally beneficial alleles are simply neutral elsewhere, a process thought to be more common when overall levels of gene flow are low (Wadgyamar *et al.* 2022) but one that could nonetheless augment the rangewide spread of such alleles.

We found a similar pattern from our analysis of shared versus unique selective sweeps, which were more often shared by at least one other allopatric population. Similar to our predictions for  $\alpha$ , we expected that local adaptation would lead most sweeps to be exclusive to individual populations. Instead, the average proportion of sweeps exclusive to a single population was low to moderate for maize and teosinte populations, respectively (Figure 4). We also expected that maize and teosinte populations growing in close proximity would share similar local selective pressures and would therefore share more signatures of adaptation. However, no pairs showed evidence of sharing more sweeps than would be expected by chance, and overall sympatric pairs did not show increased sharing of selective sweep regions compared to allopatric pairs (Figure 4). This regional scale of local adaptation is consistent with patterns seen in maize adaptation to the highlands (Calfee *et al.* 2021), where sympatric maize and teosinte populations show little evidence of adaptive gene flow, and adaptive teosinte introgression appears widespread among highland maize.

There are a number of considerations to make in the interpretation of our results. The two methods we used to identify signatures of adaptation, estimating  $\alpha$  and identifying signatures of selective sweeps, are best-suited for adaptation that leads to fixation of beneficial alleles, and/or mutations of large effect. For the moderate population sizes and selection coefficients observed here, fixation of new beneficial mutations takes a considerable amount of time, on the order of  $4\log(2N)/s$  generations (Charlesworth 2020). Compared to the sojourn time of adaptive mutations, our populations may have occupied their current locations for relatively few generations. As a result, the selective sweeps underlying local adaptation to the selective pressures that populations currently face are more likely to be incomplete, so may be more difficult to detect (Xue *et al.* 2021; Pritchard *et al.* 2010). Likewise, the adaptive sweeps that have completed may have been under selection in ancestral populations that occupied different environments than the sampled individuals, and their signatures may no longer be detectable (Przeworski 2002), placing a limit on the temporal resolution with which we can make inference about instances of local adaptation. Another complication in detecting local adaptation relates to the

size and complexity of plant genomes. Large genomes may lead to more soft sweeps, where no single mutation driving adaptive evolution would fix (Mei *et al.* 2018). Like incomplete sweeps, soft sweeps are harder to identify (Schridder and Kern 2016; Pritchard *et al.* 2010), which could obscure the signatures of local adaptation. Even if our populations have occupied their current locations for a sufficient duration for local adaptation to occur, the completion of selective sweeps may be hindered by changes and fluctuations in the local biotic and abiotic conditions. Relatively rapid change in local conditions could also result in fluctuating selection, such that most alleles do not remain beneficial for long enough to become fixed (Rudman *et al.* 2021).

While our focus has been on the trajectory of individual beneficial alleles, the genetic basis of many adaptive traits may be highly polygenic. Allele frequency changes underlying polygenic adaptation are more subtle than those assumed under selective sweeps, making them harder to detect (Pritchard *et al.* 2010). Evaluating local adaptation in maize and other systems will be facilitated by studying the contribution of polygenic adaptation to the evolution of complex traits. However, if adaptation across our studied populations were strictly polygenic, and especially if it were acting on alleles with small effect sizes, we would expect to find few to no shared sweeps. The fact that we find many instances of sharing across populations supports that a non-trivial amount of local adaptation is occurring via selective sweeps, or through polygenic adaptation acting on a few loci with large effects that leave a signature similar to that of a selective sweep.

#### **Differences in diversity and demography influence adaptation in maize and teosinte**

While our results were generally similar between the two subspecies and among the sampled populations, there are several important differences. The most obvious difference between the subspecies is the ongoing interaction and dependence of maize on humans via domestication and farming. Compared to teosinte, maize had lower average genomewide estimates of diversity (Figure 2A). These differences are consistent with the previously discovered pattern that diversity tends to be lower in crops compared to their wild relatives (Doebly 1989; Hufford *et al.* 2012), a pattern putatively driven by domestication bottlenecks (Eyre-Walker *et al.* 1998). In line with this argument, the few teosinte populations with lower diversity than those in maize (El Rodeo and San Lorenzo) were inferred to have the most substantial bottlenecks and historical inbreeding (Figure 2). More generally, we found that  $\pi$  and Tajima's D were more variable among teosinte populations, indicative of differences in their demographic histories.

Our demographic inferences suggest that all populations had signatures of a bottleneck, the timing of which coincides with the beginning of maize domestication  $\approx$  9,000 years ago (Piperno *et al.* 2009). The severity of the bottleneck varied considerably across populations, particularly for teosinte. While finding a bottleneck in the maize populations is consistent with domestication, it is less clear why we found a similar bottlenecks for the teosinte populations at approximately the same time. One possibility is that the teosinte bottlenecks reflect land use change induced by human colonization. For example, evidence from Mesoamerican phytolith records in lake sediment show evidence of anthropogenic burning as early as 11K years B.P. (Piperno 1991). The establishment and spread of human populations



479 over the subsequent millenia would require an ever increasing  
480 area for farming, dwellings, transportation, and trade (Haines  
481 *et al.* 2000). Such land use changes would likely encroach on  
482 the habitat available for teosinte and drive species-wide cen-  
483 sus size declines. Given the success of maize breeding and  
484 domestication, we anticipated a recent expansion for maize pop-  
485 ulations as previously seen (Beissinger *et al.* 2016; Wang *et al.*  
486 2017). However, with only 10 individuals per population, recent  
487 expansions will be difficult to detect with approaches based on  
488 the site frequency spectrum (Keinan and Clark 2012; Coventry  
489 *et al.* 2010). The demography of the rangewide samples for both  
490 subspecies showed little evidence of the bottleneck inferred in in-  
491 dividual populations, likely due to the reduced sampled size (5  
492 and 6 individuals) for the rangewide data. We additionally used  
493 strong regularization penalties to avoid over-fitting (see Meth-  
494 ods), which limits the detection of rapid and dramatic changes  
495 in population size. The near-constant size of the rangewide sam-  
496 ples and the lack of recent expansion in maize are both likely  
497 influenced by this modeling choice.

498 Finally, demographic inferences are known to be sensitive  
499 to the effects of linked selection (Ewing and Jensen 2016), and  
500 our demographic models have likely underestimated effective  
501 population sizes and the variation in changes over time therein.  
502 However, all populations independently converged to similar  
503 values in the oldest generation times, around the time when we  
504 would expect the ancestral lineages would have coalesced (Fig-  
505 ure 2C). This suggests any biases in the estimated population  
506 sizes that are specific to maize, which has had recent explo-  
507 sive population growth, are occurring in the more recent past  
508 (Beissinger *et al.* 2016). Similarly, although the asymptotic MK  
509 method we employed has been shown to provide reliable esti-  
510 mates of  $\alpha$  when fixations are due to strong beneficial mutations  
511 (Messer and Petrov 2013), it does not account for the influence of  
512 background selection and the rate of fixation of weakly beneficial  
513 mutations (Uricchio *et al.* 2019).

514 Differences in adaptation between maize and teosinte, and  
515 among populations, were apparent based on differences in the  
516 patterns of selective sweeps. Maize had a higher proportion  
517 of selective sweeps shared with at least one other population  
518 (Figure 4). The greater number of shared sweeps in maize popu-  
519 lations is likely the result of their recent shared selective history  
520 during the process of domestication, resulting in a set of phe-  
521 notypes common to all maize (Stützer and Ross-Ibarra 2018). In  
522 comparison, the higher proportion of unique sweeps in teosinte  
523 suggests local adaptation has played more of a role in shap-  
524 ing their recent evolutionary history. Teosinte grows untended,  
525 and did not undergo domestication, leaving more opportunity  
526 for divergence and local selection pressures to accumulate dif-  
527 ferences among populations. This is reflected in the inferred  
528 population history, which had longer terminal branch lengths  
529 for teosinte (Figure 1B), suggesting there is increased genetic  
530 isolation among teosinte populations due to longer divergence  
531 times, reduced gene flow, or both.

### 532 **Convergent adaptation is ubiquitous**

533 We found convergent adaptation to be common among popu-  
534 lations and subspecies (Figures 4 and 5). The frequency of  
535 convergence further suggests there are a large number of muta-  
536 tions that are beneficial in more than one population, even when  
537 placed in the different genomic backgrounds of the two sub-  
538 species. Our approach allowed us to distinguish between multi-  
539 ple potential modes of convergence, including a neutral model

540 that models allele frequency covariance by drift alone (Lee and  
541 Coop 2017). The distribution of most likely selection coefficients  
542 of the inferred beneficial alleles suggests the strength of selection  
543 is moderate to strong, though this estimate is likely biased as  
544 strong positive selection will be easier to detect. Convergence  
545 via independent mutations was by far the least frequent mode.  
546 This is consistent with previous analyses of domestication (Huf-  
547 ford *et al.* 2012) and adaptation (Wang *et al.* 2021) in maize, and  
548 unsurprising given evidence for ongoing gene flow (Figure 1E),  
549 the relatively short evolutionary time scales, and the low proba-  
550 bility that even strongly selected new mutations can overcome  
551 drift multiple times independently.

552 For convergent sweeps that occurred via standing variation  
553 within maize or shared between maize and teosinte, the distribu-  
554 tion of generation times that the selected variant was standing  
555 before the onset of selection tended to be bimodal, with both  
556 long and short standing times. In contrast, sweeps exclusive to  
557 teosinte were consistently inferred to be standing variation for  
558 more generations (Figure 5E). Sweeps that occurred via standing  
559 variation and shared between subspecies were often found in  
560 only a subset of maize populations. Many of these sweeps likely  
561 reflect the presence of structure in ancestral populations, sug-  
562 gesting different alleles beneficial to maize were likely derived  
563 from more than one teosinte population. The bimodal features  
564 of sharing seem at face value surprising. How can an allele be  
565 standing variation for so many generations after divergence but  
566 prior to selection when the populations diverged less than ten  
567 thousand generations ago? We speculate that ancestral popu-  
568 lation structure and limited sampling of 6 populations could  
569 explain the pattern. For example, extremely long standing times  
570 that predate domestication may reflect divergence between our  
571 sampled teosinte populations and the populations most closely  
572 related to those that gave rise to domesticated maize. This is yet  
573 another area in which more comprehensive sampling could help  
574 resolve patterns of local adaptation.

575 The most common mode of convergent adaptation was via  
576 migration, and frequently occurred between geographically dis-  
577 parate populations (Figures S6). This included a relatively large  
578 number of shared sweeps via migration between maize and  
579 teosinte (Figures 5 and S7). There is ample evidence that maize  
580 and teosinte are capable of hybridizing (Wilkes *et al.* 1967; Ell-  
581 strand *et al.* 2007; Ross-Ibarra *et al.* 2009), and previous work has  
582 identified gene flow between geographically disparate popula-  
583 tions of maize and *Zea mays mexicana* (Calfee *et al.* 2021). Further,  
584 convergence via migration between geographically disparate  
585 maize populations has been inferred during adaptation to high  
586 elevations (Wang *et al.* 2021).

587 Our findings on convergence via migration point to an in-  
588 triguing hypothesis, namely, that some number of alleles that  
589 are beneficial to teosinte may have originally arisen in another  
590 teosinte and maize populations and moved between populations  
591 via gene flow with maize, an idea suggested by Ross-Ibarra *et al.*  
592 (2009) based on allele sharing at a small set of loci. Our inference  
593 that migration is a frequent source of beneficial alleles in teosinte  
594 populations suggests that they may be mutation limited. Con-  
595 sistent with this, the three teosinte populations that most often  
596 shared sweeps with maize (El Rodeo, San Lorenzo, and Amatlán  
597 de Cañas) (Figure S7) also showed the strongest signatures of  
598 bottlenecks (Figure 2C), which would limit the rate of new and  
599 beneficial mutations. It is worth noting that the total number of  
600 shared sweeps is much lower than previously reported (Tittes  
601 *et al.* 2021), and only four of fifteen instances of convergence via



migration include two or more teosinte and maize populations (Figure S7). Despite the lower totals, the evidence still supports this hypothesis. Firstly, we found relatively few shared sweeps exclusive to teosinte populations (Figure 5C), which is what we would expect if maize populations facilitate the movement of beneficial teosinte alleles. However, it is important to note that there are fewer sweeps exclusive to teosinte for all modes of convergence, not just via migration, so this alone is not sufficient evidence. Thirdly, sweeps shared via migration that were exclusive to teosinte were always inferred to be the lowest migration rate ( $1 \times 10^{-3}$ ) (Figure 5F), where those shared by both subspecies or exclusive to maize were primarily inferred to be the highest migration rate ( $1 \times 10^{-1}$ ). This indicates alleles that are only beneficial in teosinte move between populations more slowly. Despite the patterns of population structure in both subspecies, there is evidence of gene flow based on f4 tests. In particular, f4 tests that included maize from Crucero Lagunitas were consistently elevated across both subspecies (Figure 1E and S1). This is in accordance with our finding that Crucero Lagunitas maize was one of the most commonly inferred source populations of migration sweeps that were shared between maize and teosinte (Figure 5D). Together, these results suggests that geographically widespread varieties of maize such as Celaya (Crucero Lagunitas) (Orozco-Ramírez *et al.* 2017) may have played a prominent role as a source of and/or transport for beneficial alleles among maize and teosinte populations. However, teosinte populations were often the source of beneficial alleles for sweeps shared between both subspecies (Figure 5C). As such, teosinte populations may have also commonly been the source of adaptive variation for both other teosinte and maize populations.

## Materials and Methods

### Samples and whole genome resequencing

We sampled seeds from five populations of *Zea mays* ssp. *parviglumis* and four populations of *Zea mays* ssp. *mays* from plants growing across the species' native range. We additionally included populations of *parviglumis* and maize from Palmar Chico which were previously analyzed and reported in (Chen *et al.* 2020) for a total of 6 and 5 populations of maize and teosinte (See Supplement I for accession IDs and further sample details). All maize and teosinte populations from each named location were less than 1km from one another, with the exception of Crucero Lagunitas, which were separated by approximately 18km.

DNA extraction for teosinte followed (Chen *et al.* 2020). Genomic DNA for landraces was extracted from leaf tissue using the E.Z.N.A.® Plant DNA Kit (Omega Biotek), following manufacturer's instructions. DNA was quantified using a Qubit (Life Technologies) and 1ug of DNA per individual was fragmented using a bioruptor (Diagenode) with 30 seconds on/off cycles.

DNA fragments were then prepared for Illumina sequencing. First, DNA fragments were repaired with the End-Repair enzyme mix (New England Biolabs). A deoxyadenosine triphosphate was added at each 3' end with the Klenow fragment (New England Biolabs). Illumina Truseq adapters (Affymetrix) were then added with the Quick ligase kit (New England Biolabs). Between each enzymatic step, DNA was washed with sera-mags speed beads (Fisher Scientific). The libraries were sequenced to an average coverage of 20 to 25x PE150 on the Xten at Novogene (Sacramento, USA).

We additionally grew one individual of *Zea diploperennis* from the UC Davis Botanical Conservatory as an outgroup. DNA for *Zea diploperennis* was extracted and libraries prepared as above,

and then sequenced to 60X coverage using PE250 on 3 lanes of Illumina 2000 rapid run (UC Davis Genome Center, Davis, USA).

Sequencing reads have been deposited in the NCBI Sequence Read Archive under project number (to be submitted).

### Sequencing and variant identification

All paired-end reads were aligned to version 5 of the maize B73 reference genome (Hufford *et al.* 2021) using bwa-mem (v0.7.17) (Li 2013). Default options were used for mapping except -M to enable marking short hits as secondary, -R for providing the read group, and -K 10000000, for processing 10 Mb input in each batch. Sentieon (v201808.01) (Freed *et al.* 2017) was used to process the alignments to remove duplicates (option -algo Dedup) and to calculate various alignment metrics (GC bias, MQ value distribution, mean quality by cycle, and insert size metrics) to ensure proper mapping of the reads.

All downstream analyses were based on genotype likelihoods estimated with ANGSD (v0.934) (Korneliussen *et al.* 2014) using the following command line flags and filters:

```
-GL 1
-P 5
-uniqueOnly 1
-remove_bads 1
-only_proper_pairs 1
-trim 0
-C 50
-minMapQ 30
-minQ 30
```

### Genetic Diversity

We estimated per base nucleotide diversity ( $\pi$ ) and Tajima's D ( $D$ ) in non-overlapping 1kb, 100kb and 1,000kb windows with the *thetaStat* utility from ANGSD, though estimates did not substantively differ between window sizes. To estimate  $\pi$  and the unfolded site frequency spectra for each population, we polarized alleles as ancestral and derived using short-read sequence data for *Zea luxurians* and *Zea diploperennis* as outgroups. *Zea luxurians* sequence from Tenaillon *et al.* (2011) was downloaded from The NCBI Sequence Read Archive (study SRR088692). We used the alignments from the two species to make minor allele frequency (MAF) files using ANGSD. We used the MAF files to construct a table of genotypes found at each locus. Sites with minor allele frequency estimates greater than 0.001 were treated as heterozygous. Sites that were homozygous in both species were imputed onto the maize v5 reference and assumed to be the ancestral allele. As there were substantially more called bases in *Zea luxurians* than in *Zea diploperennis*, we also assumed sites that were homozygous in *luxurians* and missing in *diploperennis* were ancestral, but excluded sites that were missing from *luxurians*. Sites that were classified as heterozygous were treated as missing and imputed onto the maize reference as 'N'.

### Population Structure and Introgression

We used *ngsadmix* (Skotte *et al.* 2013) to assess population structure within subspecies. To do so we used a SNP-calling procedure in ANGSD with the same filters as listed above, along with a SNP p-value cutoff of  $1 \times 10^{-6}$ . We looked for evidence of gene flow between subspecies using f4 statistics and Z-scores calculated with blocked jackknifing, implemented using treemix (Pickrell and Pritchard 2012). Trees for f4 tests were always of the form (*Maize\_X*, *Maize\_Y*; *Teosinte\_focal*, *Teosinte\_Z*), or (*Maize\_focal*, *Maize\_Y*; *Teosinte\_W*, *Teosinte\_Z*); with each unique combination of populations was considered to be the "focal" and "\_X" positions of the tree. We considered any tree with a Z-score greater than or equal to 3 significant, indicating a departure from the allele frequency differences expected if population history matched the hypothesized tree. We assessed Z-scores separately based on whether the focal population was maize or teosinte, and for trees that include the sympatric pair of the focal population.

### Demographic and Inbreeding History

We inferred each population's demography using a single unfolded site frequency spectrum with mushi (v0.2.0) (DeWitt *et al.* 2021). In efforts to reduce overfitting given our modest samples sizes, we increased the



regularization penalty parameters to  $\alpha_{tv}=1e4$ ,  $\alpha_{spline}=1e4$ , and  $\alpha_{ridge} = 1e-1$ .

We assessed homozygosity by descent (HBD) in each population using IBDseq (v2.0) (Browning and Browning 2013). We compared empirical results to simulations in msprime (Kelleher et al. 2016) using each population's inferred demographic history. We performed ten replicates of each of these simulations. Replicates were similar across all populations; only one replicate was chosen at random for visual clarity. We estimated recent inbreeding using ngsrelate (Hanghoj et al. 2019) with default parameters. Input files were generated using ANGSD with the same filters as listed above, along with a SNP p value cutoff and maf filter of

```
-SNP_pval 1e-6
-minmaf 0.05,
```

respectively.

#### Estimating the Rate of Positive Selection, $\alpha$

We modeled the rate of positive selection,  $\alpha$  of 0-fold nonsynonymous mutations using the asymptotic extension of the McDonald-Kreitman (MK) test (Messer and Petrov 2013), where  $\alpha$  is calculated at each allele frequency bin of the uSFS (from  $1/n$  to  $(n-1)/n$ ). At each allele frequency bin, each  $\alpha$  was calculated as

$$\alpha = 1 - \frac{d_0}{d} \frac{p}{p_0}$$

where  $d_0$  and  $d$  are the number of derived fixed differences for selected and putatively neutral sites, respectively, and  $p_0$  and  $p$  are the number of selected and putatively neutral polymorphic sites. We identified 0-fold and 4-fold sites using Python ([https://github.com/silastittes/cds\\_fold](https://github.com/silastittes/cds_fold)). We fit the Asymptotic MK extension as a nonlinear Bayesian mixed-model using the R package *brms* (Bürkner 2017, 2018).

$$\alpha_{ij} \sim a_j + b_j e^{-c_j x_{ij}}$$

where  $\alpha_{ij}$  is the value of  $\alpha$  calculated at the  $i^{\text{th}}$  allele frequency bin of the  $j^{\text{th}}$  population and  $x_{ij}$  is the corresponding allele frequency bin. The nonlinear *brms* model was coded as

```
alpha ~
  a + b * exp(-c * allele_frequency)
```

where all three free parameters of the asymptotic function ( $a$ ,  $b$ , and  $c$ ) were treated as random effects of population and nucleotide type (see Supplement III), and the subspecies was treated as a fixed effect. These effects were coded in *brms* as

```
a + b + c ~
  1 + allele_frequency +
  (1 + allele_frequency | pop) +
  (1 + allele_frequency | nuc_type) +
  ssp
```

#### Identifying Selective Sweeps

We used RAiSD (Alachiotis and Pavlidis 2018) to infer signatures of selective sweeps in each population, including the rangewide samples. Across all populations, we used a minor allele frequency threshold of 0.05 and a window size of 24 SNPs. We called SNPs and generated VCF files for each population using the *dovcf* utility from ANGSD, using a SNP calling p-value cut off of  $1 \times 10^{-6}$ . We used the Python package *mop* (<https://pypi.org/project/mop-bam/>) to exclude SNPs that fell in regions with low and excessive coverage and/or poor quality. Here we required each locus to have at least 70% of individuals with a depth between 5 and 100, and to have a phred scaled quality scores above 30 for base and mapping quality. We additionally used *mop* to rescale the  $\mu_{var}$  sub-statistic in each population based on the proportion of high quality bases available in each of the RAiSD SNP windows, after which we recalculated the overall  $\mu$  statistic as the product of the three sub-statistics (Alachiotis and Pavlidis 2018).

Individual SNP windows in RAiSD are small and spatially auto-correlated with neighboring windows, implying that a sweep signature is distributed over multiple windows. This makes it difficult to compare shared RAiSD outliers across populations, which may have experienced the same sweep, but may differ in how the  $\mu$  statistic is distributed across windows. To compare sweep signatures across populations we collected

outliers into "sweep regions" by fitting a cubic spline modeling the adjusted  $\mu$  statistic by position along the chromosome using *smooth.spline* function in R, which uses cross validation to choose the optimal smoothing parameter for the cubic spline. We compared the empirical cubic spline fit to the those simulated under each populations' demography using *msprime* (Kelleher et al. 2016), and selected windows with fitted values greater than 99.9th percentile from the simulations as outlier regions. We merged outlier regions within 50,000 Kb of one another and treated as a single sweep region. The custom R functions for a defining outlier regions is available at [https://github.com/silastittes/sweep\\_regions](https://github.com/silastittes/sweep_regions).

For the above steps, we selected the best combination of parameters by conducting a grid search that optimized on the highest proportion of sweeps shared between the two Palmar Chico replicates, averaged over both subspecies. For the grid search we considered RAiSD snp windows of 10, 24, 50, 100, 200, and 500; outlier quantiles of 0.8, 0.9, 0.95, 0.99, and 0.999; and merge windows of 50K, 100K, 200K, and 500K BPs.

#### Assessing the precision of sweep inferences and the number of shared sweeps expected by chance

To assess precisions of sweep inferences, we used a second random sample of non-overlapping individuals from the two Palmar Chico populations. False positives were assessed based on the number of sweep regions that did not overlap between the 2 replicate Palmar Chico samples from each subspecies. To account for differences in the total number of sweep regions for each replicate, we averaged the two proportions

$$P = 1 - \left( \frac{n_S}{n_{P1}} + \frac{n_S}{n_{P2}} \right) / 2$$

where  $n_S$  is the number of sweeps shared between the replicates, and  $n_{P1}$  and  $n_{P2}$  were the number of sweeps in the first and second replicates, respectively. In downstream analyses, we used the average value of  $P$  for the two subspecies, although it was higher for teosinte than for maize (0.67 and 0.80, respectively).

We evaluated the number of sweeps that we would expect populations to share by chance using a simple statistical test based on the hypergeometric distribution,

$$Pr(x \geq X) = \sum_{x \geq X} \frac{\binom{n_2}{x} \binom{N}{n_1 - x}}{\binom{N}{n_1}}$$

where  $N$  is the total number of loci tested;  $n_1$  and  $n_2$  are the number of outlier loci in the first and second populations, respectively; and  $x$  is the number of shared outliers between the two populations. The population with the larger number of outliers was always designated at the first population. We accounted for false positive by multiplying the raw values of  $N$ ,  $n_1$ ,  $n_2$ , and  $x$  by the *FP* value described above.

We corrected p-values for multiple tests using the Benjamini and Yekutieli method implemented with the R function *p.adjust* (Benjamini and Yekutieli 2001).

#### Inferring modes of convergent adaptation

For sweep regions that were overlapping in 2 to 9 of the 11 populations, we used *rdmc* to infer the most likely mode of convergent adaptation (Lee and Coop 2017; Tittes 2020). To ensure a sufficient number of loci were included to estimate decay in covariance across the sweep regions, we added 10% of each sweep region's total length on each of its ends prior to fitting the models. To reduce the computation time, we exclude sites that had an allele frequency less than 1/20 across all populations. As sweep regions differed in size, we subset from their total number of sites to maintain approximately similar densities, with a lower and upper bound of 1K and 100K SNPs, respectively. Sweep regions near the ends of chromosomes for which we could not estimate the number of centiMorgans for were subset to 10K SNPs. To contrast allele frequency covariance in sweep regions to neutral expectations, we first sampled allele frequencies at 100K random loci. When fitting *rdmc*, we assumed the effective population size was 50K for all populations. The recombination rate was approximated for each sweep region as the median interpolated value based on a previously generated genetic map for maize that was lifted on to the v5 reference genome (Ogut et al. 2015). The *rdmc* function includes arguments that control the grid of parameter values over which composite likelihoods were computed were:

```
n_sites = 20,
num_bins = 1000,
sels = 10~seq(-5, -1, length.out = 15),
times = c(1e2, 1e3, 1e4, 1e5),
```



```
861 gs = 10-seq(-3, -1, length.out = 3),
862 migs = 10^(seq(-3, -1, length.out = 2)),
863 cholesky = TRUE
```

864 We compared composite likelihoods over four convergent adaptation  
865 modes, "neutral", "independent", "standing", and "migration". We  
866 assigned each sweep to the mode with the highest log composite likeli-  
867 hood. To assess the overall performance of the method to distinguish  
868 between the four modes, we computed differences between the highest  
869 composite likelihood and the next highest for each sweep.

870 All wrangling to prepare input data for statistical analyses was done  
871 using R (R Core Team 2020) with appreciable reliance on functions  
872 from the tidyverse suite (Wickham *et al.* 2019). Figures were made  
873 using ggplot2 (Wickham 2016), patchwork (Pedersen 2019), and cow-  
874 plot (Wilke 2019). Bam files that all downstream analyses are based  
875 on are available <https://datacommons.cyverse.org/browse/iplant/home/aseetharam/B73v5-deduped-alignments>. The processed data used for  
876 generating figures and analyses are available from [https://datacommons.cyverse.org/browse/iplant/home/silasittes/parv\\_local\\_data](https://datacommons.cyverse.org/browse/iplant/home/silasittes/parv_local_data). Code and in-  
877 structions for the entirety of the analyses, including Jupyter notebooks  
878 for reproducing figures, is available from [https://github.com/silasittes/parv\\_local](https://github.com/silasittes/parv_local).

## 882 Acknowledgments

883 We would like to thank Andi Kur for providing the corn art, along with  
884 Matthew Gibson, Tom Booker, Cathy Rushworth, and other members  
885 of the Ross-Ibarra lab for feedback and suggestions on early drafts of  
886 the manuscript. This work was funded in part by grants from the  
887 National Science Foundation (1822330 and 1238014). We would also like  
888 to acknowledge Felix Andrews for statistical advice, although we did  
889 not follow it.

## 890 References

891 Aguirre-Liguori, J. A., B. S. Gaut, J. P. Jaramillo-Correa, M. I. Tenaillon,  
892 S. Montes-Hernández, *et al.*, 2019 Divergence with gene flow is driven  
893 by local adaptation to temperature and soil phosphorus concentration  
894 in teosinte subspecies (*zea mays parviglumis* and *zea mays mexicana*).  
895 *Molecular ecology* **28**: 2814–2830.  
896 Alachiotis, N. and P. Pavlidis, 2018 Ralds detects positive selection based  
897 on multiple signatures of a selective sweep and snp vectors. *Communi-*  
898 *cations biology* **1**: 1–11.  
899 Beissinger, T. M., L. Wang, K. Crosby, A. Durvasula, M. B. Hufford, *et al.*,  
900 2016 Recent demography drives changes in linked selection across  
901 the maize genome. *Nature plants* **2**: 1–7.  
902 Bellon, M. R., A. Mastretta-Yanes, A. Ponce-Mendoza, D. Ortiz-  
903 Santamaría, O. Oliveros-Galindo, *et al.*, 2018 Evolutionary and food  
904 supply implications of ongoing maize domestication by mexican  
905 campesinos. *Proceedings of the Royal Society B* **285**: 20181049.  
906 Benjamini, Y. and D. Yekutieli, 2001 The control of the false discovery  
907 rate in multiple testing under dependency. *Annals of statistics* pp.  
908 1165–1188.  
909 Bourne, E. C., G. Bocedi, J. M. Travis, R. J. Pakeman, R. W. Brooker,  
910 *et al.*, 2014 Between migration load and evolutionary rescue: dispersal,  
911 adaptation and the response of spatially structured populations to  
912 environmental change. *Proceedings of the Royal Society B: Biological*  
913 *Sciences* **281**: 20132795.  
914 Browning, B. L. and S. R. Browning, 2013 Detecting identity by descent  
915 and estimating genotype error rates in sequence data. *The American*  
916 *Journal of Human Genetics* **93**: 840–851.  
917 Buckler, E. and T. P. Holtsford, 1996 *Zea* systematics: ribosomal its  
918 evidence. *Molecular Biology and Evolution* **13**: 612–622.  
919 Butler, E. E. and P. Huybers, 2013 Adaptation of us maize to temperature  
920 variations. *Nature Climate Change* **3**: 68–72.  
921 Bürkner, P.-C., 2017 brms: An R package for Bayesian multilevel models  
922 using Stan. *Journal of Statistical Software* **80**: 1–28.  
923 Bürkner, P.-C., 2018 Advanced Bayesian multilevel modeling with the R  
924 package brms. *The R Journal* **10**: 395–411.  
925 Calfee, E., D. Gates, A. Lorant, M. T. Perkins, G. Coop, *et al.*, 2021 Selec-  
926 tive sorting of ancestral introgression in maize and teosinte along an  
927 elevational cline. *bioRxiv* .  
928 Charlesworth, B., 2020 How long does it take to fix a favorable mutation,  
929 and why should we care? *The American Naturalist* **195**: 753–771.  
930 Chen, Q., L. F. Samayoa, C. J. Yang, P. J. Bradbury, B. A. Olukolu, *et al.*,  
931 2020 The genetic architecture of the maize progenitor, teosinte, and

932 how it was altered during maize domestication. *PLoS genetics* **16**:  
933 e1008791.  
934 Chevin, L.-M., G. Martin, and T. Lenormand, 2010 Fisher's model and the  
935 genomics of adaptation: restricted pleiotropy, heterogenous mutation,  
936 and parallel evolution. *Evolution: International Journal of Organic*  
937 *Evolution* **64**: 3213–3231.  
938 Clark, R. M., S. Tavaré, and J. Doebley, 2005 Estimating a nucleotide sub-  
939 stitution rate for maize from polymorphism at a major domestication  
940 locus. *Molecular biology and evolution* **22**: 2304–2312.  
941 Clausen, J., D. D. Keck, W. M. Hiesey, *et al.*, 1948 Experimental studies on  
942 the nature of species. iii. environresponses of climatic races of achillea.  
943 Experimental studies on the nature of species. III. Environresponses  
944 of climatic races of Achillea. .  
945 Colosimo, P. F., K. E. Hosemann, S. Balabhadra, G. Villarreal, M. Dickson,  
946 *et al.*, 2005 Widespread parallel evolution in sticklebacks by repeated  
947 fixation of ectodysplasin alleles. *science* **307**: 1928–1933.  
948 Coventry, A., L. M. Bull-Ottersson, X. Liu, A. G. Clark, T. J. Maxwell, *et al.*,  
949 2010 Deep resequencing reveals excess rare recent variants consistent  
950 with explosive population growth. *Nature communications* **1**: 1–6.  
951 DeWitt, W. S., K. D. Harris, A. P. Ragsdale, and K. Harris, 2021 Non-  
952 parametric coalescent inference of mutation spectrum history and  
953 demography. *Proceedings of the National Academy of Sciences* **118**.  
954 Doebley, J., 1989 Isozymic evidence and the evolution of crop plants. In  
955 *Isozymes in plant biology*, pp. 165–191, Springer.  
956 Ellstrand, N. C., L. C. Garner, S. Hegde, R. Guadagnuolo, and L. Blancas,  
957 2007 Spontaneous hybridization between maize and teosinte. *Journal*  
958 *of Heredity* **98**: 183–187.  
959 Ewing, G. B. and J. D. Jensen, 2016 The consequences of not accounting  
960 for background selection in demographic inference. *Molecular ecology*  
961 **25**: 135–141.  
962 Eyre-Walker, A., R. L. Gaut, H. Hilton, D. L. Feldman, and B. S. Gaut,  
963 1998 Investigation of the bottleneck leading to the domestication of  
964 maize. *Proceedings of the National Academy of Sciences* **95**: 4441–  
965 4446.  
966 Fournier-Level, A., A. Korte, M. D. Cooper, M. Nordborg, J. Schmitt,  
967 *et al.*, 2011 A map of local adaptation in arabidopsis thaliana. *Science*  
968 **334**: 86–89.  
969 Frachon, L., C. Libourel, R. Villoutreix, S. Carrère, C. Glorieux, *et al.*,  
970 2017 Intermediate degrees of synergistic pleiotropy drive adaptive  
971 evolution in ecological time. *Nature ecology & evolution* **1**: 1551–1561.  
972 Freed, D., R. Aldana, J. A. Weber, and J. S. Edwards, 2017 The sentieon  
973 genomics tools—a fast and accurate solution to variant calling from  
974 next-generation sequence data. *BioRxiv* p. 115717.  
975 Fustier, M.-A., J.-T. Brandenburg, S. Boitard, J. Lapeyronnie, L. Eguarte,  
976 *et al.*, 2017 Signatures of local adaptation in lowland and highland  
977 teosintes from whole-genome sequencing of pooled samples. *Molecu-*  
978 *lar Ecology* **26**: 2738–2756.  
979 Fustier, M.-A., N. E. Martínez-Ainsworth, J. A. Aguirre-Liguori,  
980 A. Venon, H. Corti, *et al.*, 2019 Common gardens in teosintes reveal the  
981 establishment of a syndrome of adaptation to altitude. *PLoS genetics*  
982 **15**: e1008512.  
983 Gates, D. J., D. Runcie, G. M. Janzen, A. R. Navarro, M. Willcox, *et al.*,  
984 2019 Single-gene resolution of locally adaptive genetic variation in  
985 mexican maize. *BioRxiv* p. 706739.  
986 Geist, K. S., J. E. Strassmann, and D. C. Queller, 2019 Family quarrels in  
987 seeds and rapid adaptive evolution in arabidopsis. *Proceedings of the*  
988 *National Academy of Sciences* **116**: 9463–9468.  
989 Gossmann, T. I., B.-H. Song, A. J. Windsor, T. Mitchell-Olds, C. J. Dixon,  
990 *et al.*, 2010 Genome wide analyses reveal little evidence for adaptive  
991 evolution in many plant species. *Molecular biology and evolution* **27**:  
992 1822–1832.  
993 Haines, M. R., M. R. Haines, and R. H. Steckel, 2000 *A population history*  
994 *of North America*. Cambridge University Press.  
995 Hämälä, T. and P. Tiffin, 2020 Biased gene conversion constrains adapta-  
996 tion in arabidopsis thaliana. *Genetics* **215**: 831–846.  
997 Hamrick, J. and R. W. Allard, 1972 Microgeographical variation in al-  
998 lozyme frequencies in avena barbata. *Proceedings of the National*  
999 *Academy of Sciences* **69**: 2100–2104.  
1000 Hanghøj, K., I. Moltke, P. A. Andersen, A. Manica, and T. S. Korneliussen,  
1001 2019 Fast and accurate relatedness estimation from high-throughput  
1002 sequencing data in the presence of inbreeding. *Gigascience* **8**: giz034.  
1003 Hufford, M. B., 2010 *Genetic and ecological approaches to guide conserva-*  
1004 *tion of teosinte (Zea mays ssp. parviglumis), the wild progenitor of maize*.  
1005 University of California, Davis.  
1006 Hufford, M. B., P. Gepts, and J. Ross-IBARRA, 2011 Influence of cryptic  
1007 population structure on observed mating patterns in the wild pro-



- 1008 genitor of maize (*zea mays* ssp. *parviglumis*). *Molecular ecology* **20**: 1084  
1009 46–55. 1085
- 1010 Hufford, M. B., A. S. Seetharam, M. R. Woodhouse, K. M. Chougule, 1086  
1011 S. Ou, *et al.*, 2021 De novo assembly, annotation, and comparative 1087  
1012 analysis of 26 diverse maize genomes. *Science* . 1088
- 1013 Hufford, M. B., X. Xu, J. Van Heerwaarden, T. Pyhäjärvi, J.-M. Chia, *et al.*, 1089  
1014 2012 Comparative population genomics of maize domestication and 1090  
1015 improvement. *Nature genetics* **44**: 808. 1091
- 1016 Janzen, G. M., M. R. Aguilar-Rangel, C. Cántora-Martínez, K. A. Blöcher- 1092  
1017 Juárez, E. González-Segovia, *et al.*, 2021 Demonstration of local adap- 1093  
1018 tation of maize landraces by reciprocal transplantation. *bioRxiv* . 1094
- 1019 Keinan, A. and A. G. Clark, 2012 Recent explosive human population 1095  
1020 growth has resulted in an excess of rare genetic variants. *science* **336**: 1096  
1021 740–743. 1097
- 1022 Kelleher, J., A. M. Etheridge, and G. McVean, 2016 Efficient coalescent 1098  
1023 simulation and genealogical analysis for large sample sizes. *PLoS* 1099  
1024 *computational biology* **12**: e1004842. 1100
- 1025 Kern, A. D. and D. R. Schrider, 2016 Discoal: flexible coalescent simula- 1101  
1026 tions with selection. *Bioinformatics* **32**: 3839–3841. 1102
- 1027 Korneliussen, T. S., A. Albrechtsen, and R. Nielsen, 2014 Angsd: analysis 1103  
1028 of next generation sequencing data. *BMC bioinformatics* **15**: 356. 1104
- 1029 Lee, K. M. and G. Coop, 2017 Distinguishing among modes of convergent 1105  
1030 adaptation using population genomic data. *Genetics* **207**: 1591–1619. 1106
- 1031 Li, H., 2013 Aligning sequence reads, clone sequences and assembly 1107  
1032 contigs with bwa-mem. *arXiv preprint arXiv:1303.3997* . 1108
- 1033 Lowry, D. B., R. C. Rockwood, and J. H. Willis, 2008 Ecological reproduc- 1109  
1034 tive isolation of coast and inland races of *mimulus guttatus*. *Evolution: International Journal of Organic Evolution* **62**: 2196–2214. 1110  
1035 1111
- 1036 Mei, W., M. G. Stetter, D. J. Gates, M. C. Stitzer, and J. Ross-Ibarra, 2018 1112  
1037 Adaptation in plant genomes: Bigger is different. 1113
- 1038 Messer, P. W. and D. A. Petrov, 2013 Frequent adaptation and the 1114  
1039 mcdonald–kreitman test. *Proceedings of the National Academy of Sciences* **110**: 8615–8620. 1115  
1040 1116
- 1041 Nannas, N. J. and R. K. Dawe, 2015 Genetic and genomic toolbox of *zea* 1117  
1042 *mays*. *Genetics* **199**: 655–669. 1118
- 1043 O'Brien, A. M., R. J. Sawers, S. Y. Strauss, and J. Ross-Ibarra, 2019 Adap- 1119  
1044 tive phenotypic divergence in an annual grass differs across biotic 1120  
1045 contexts. *Evolution* **73**: 2230–2246. 1121
- 1046 Ogut, F., Y. Bian, P. J. Bradbury, and J. B. Holland, 2015 Joint-multiple 1122  
1047 family linkage analysis predicts within-family variation better than 1123  
1048 single-family analysis of the maize nested association mapping popu- 1124  
1049 lation. *Heredity* **114**: 552–563. 1125
- 1050 Orozco-Ramírez, Q., H. Perales, and R. J. Hijmans, 2017 Geographical 1126  
1051 distribution and diversity of maize (*zea mays* l. subsp. *mays*) races in 1127  
1052 mexico. *Genetic resources and crop evolution* **64**: 855–865. 1128
- 1053 Ossowski, S., K. Schneeberger, J. I. Lucas-Lledó, N. Warthmann, R. M. 1129  
1054 Clark, *et al.*, 2010 The rate and molecular spectrum of spontaneous 1130  
1055 mutations in *arabidopsis thaliana*. *science* **327**: 92–94. 1131
- 1056 Pedersen, T. L., 2019 *patchwork: The Composer of Plots*. R package version 1132  
1057 1.0.0. 1133
- 1058 Pickrell, J. and J. Pritchard, 2012 Inference of population splits and 1134  
1059 mixtures from genome-wide allele frequency data. *Nature Precedings* 1135  
1060 pp. 1–1. 1136
- 1061 Piperno, D. R., 1991 The status of phytolith analysis in the american 1137  
1062 tropics. *Journal of World Prehistory* **5**: 155–191. 1138
- 1063 Piperno, D. R., A. J. Ranere, I. Holst, J. Iriarte, and R. Dickau, 2009 1139  
1064 Starch grain and phytolith evidence for early ninth millennium bp 1140  
1065 maize from the central balsas river valley, mexico. *Proceedings of the* 1141  
1066 *National Academy of Sciences* **106**: 5019–5024. 1142
- 1067 Portwood, J. L., M. R. Woodhouse, E. K. Cannon, J. M. Gardiner, L. C. 1143  
1068 Harper, *et al.*, 2019 Maizegdb 2018: the maize multi-genome genetics 1144  
1069 and genomics database. *Nucleic acids research* **47**: D1146–D1154. 1145
- 1070 Pritchard, J. K., J. K. Pickrell, and G. Coop, 2010 The genetics of human 1146  
1071 adaptation: hard sweeps, soft sweeps, and polygenic adaptation. 1147  
1072 *Current biology* **20**: R208–R215. 1148
- 1073 Przeworski, M., 2002 The signature of positive selection at randomly 1149  
1074 chosen loci. *Genetics* **160**: 1179–1189. 1150
- 1075 Pyhäjärvi, T., M. B. Hufford, S. Mezouk, and J. Ross-Ibarra, 2013 1151  
1076 Complex patterns of local adaptation in teosinte. *Genome biology and* 1152  
1077 *evolution* **5**: 1594–1609. 1153
- 1078 R Core Team, 2020 R: *A Language and Environment for Statistical Computing*. 1154  
1079 R Foundation for Statistical Computing, Vienna, Austria. 1155
- 1080 Ranum, P., J. P. Peña-Rosas, and M. N. Garcia-Casal, 2014 Global maize 1156  
1081 production, utilization, and consumption. *Annals of the new York* 1157  
1082 *academy of sciences* **1312**: 105–112.
- 1083 Rodriguez-Zapata, F., A. C. Barnes, K. A. Blocher-Juarez, D. J. Gates, 1158  
1084 A. Kur, *et al.*, 2021 Teosinte introgression modulates phosphatidyl- 1159  
1085 choline levels and induces early maize flowering time. *bioRxiv* . 1160
- 1086 Ross-Ibarra, J., M. Tenaillon, and B. S. Gaut, 2009 Historical divergence 1161  
1087 and gene flow in the genus *zea*. *Genetics* **181**: 1399–1413. 1162
- 1088 Rudman, S. M., S. I. Greenblum, S. Rajpurohit, N. J. Betancourt, J. Hanna, 1163  
1089 *et al.*, 2021 Direct observation of adaptive tracking on ecological 1164  
1090 timescales in *drosophila*. *bioRxiv* . 1165
- 1091 Savolainen, O., M. Lascoux, and J. Merilä, 2013 Ecological genomics of 1166  
1092 local adaptation. *Nature Reviews Genetics* **14**: 807–820. 1167
- 1093 Schrider, D. R. and A. D. Kern, 2016 S/hic: robust identification of soft 1168  
1094 and hard sweeps using machine learning. *PLoS genetics* **12**: e1005928. 1169
- 1095 Skotte, L., T. S. Korneliussen, and A. Albrechtsen, 2013 Estimating indi- 1170  
1096 vidual admixture proportions from next generation sequencing data. 1171  
1097 *Genetics* **195**: 693–702. 1172
- 1098 Smith, N. G. and A. Eyre-Walker, 2002 Adaptive protein evolution in 1173  
1099 *drosophila*. *Nature* **415**: 1022–1024. 1174
- 1100 Stitzer, M. C. and J. Ross-Ibarra, 2018 Maize domestication and gene 1175  
1101 interaction. *New phytologist* **220**: 395–408. 1176
- 1102 Swarts, K., R. M. Gutaker, B. Benz, M. Blake, R. Bukowski, *et al.*, 2017 Ge- 1177  
1103 nomic estimation of complex traits reveals ancient maize adaptation 1178  
1104 to temperate north america. *Science* **357**: 512–515. 1179
- 1105 Tenaillon, M. I., M. B. Hufford, B. S. Gaut, and J. Ross-Ibarra, 2011 1180  
1106 Genome size and transposable element content as determined by 1181  
1107 high-throughput sequencing in maize and *zea luxurians*. *Genome* 1182  
1108 *biology and evolution* **3**: 219–229. 1183
- 1109 Tittes, S., 2020 rdmcm: an open source r package implementing conver- 1184  
1110 gent adaptation models of lee and coop (2017). *G3: Genes, Genomes,* 1185  
1111 *Genetics* **10**: 3041–3046. 1186
- 1112 Tittes, S., A. Lorant, S. McGinty, J. F. Doebley, J. B. Holland, *et al.*, 2021 1187  
1113 Not so local: the population genetics of convergent adaptation in 1188  
1114 maize and teosinte (version 1). *bioRxiv* . 1189
- 1115 Tuanmu, M.-N. and W. Jetz, 2015 A global, remote sensing-based char- 1190  
1116 acterization of terrestrial habitat heterogeneity for biodiversity and 1191  
1117 ecosystem modelling. *Global Ecology and Biogeography* **24**: 1329– 1192  
1118 1339. 1193
- 1119 Uricchio, L. H., D. A. Petrov, and D. Enard, 2019 Exploiting selection 1194  
1120 at linked sites to infer the rate and strength of adaptation. *Nature* 1195  
1121 *ecology & evolution* **3**: 977–984. 1196
- 1122 Van Heerwaarden, J., J. ROSS-IBARRA, J. Doebley, J. C. Glaubitz, 1197  
1123 J. DE JESÚS SÁNCHEZ GONZÁLEZ, *et al.*, 2010 Fine scale genetic 1198  
1124 structure in the wild ancestor of maize (*zea mays* ssp. *parviglumis*). 1199  
1125 *Molecular Ecology* **19**: 1162–1173. 1200
- 1126 Wadgymer, S. M., M. L. DeMarche, E. B. Josephs, S. N. Sheth, and J. T. 1201  
1127 Anderson, 2022 Local adaptation: Causal agents of selection and 1202  
1128 adaptive trait divergence. *Annual Review of Ecology, Evolution, and* 1203  
1129 *Systematics* **53**: 87–111. 1204
- 1130 Wang, L., T. M. Beissinger, A. Lorant, C. Ross-Ibarra, J. Ross-Ibarra, 1205  
1131 *et al.*, 2017 The interplay of demography and selection during maize 1206  
1132 domestication and expansion. *Genome biology* **18**: 1–13. 1207
- 1133 Wang, L., E. B. Josephs, K. M. Lee, L. M. Roberts, R. Rellán-Álvarez, *et al.*, 1208  
1134 2021 Molecular parallelism underlies convergent highland adaptation 1209  
1135 of maize landraces. *Molecular biology and evolution* **38**: 3567–3580. 1210
- 1136 Whitehead, A., F. Galvez, S. Zhang, L. M. Williams, and M. F. Olek- 1211  
1137 siak, 2011 Functional genomics of physiological plasticity and local 1212  
1138 adaptation in killifish. *Journal of Heredity* **102**: 499–511. 1213
- 1139 Wickham, H., 2016 *ggplot2: Elegant Graphics for Data Analysis*. Springer- 1214  
1140 Verlag New York. 1215
- 1141 Wickham, H., M. Averick, J. Bryan, W. Chang, L. D. McGowan, *et al.*, 1216  
1142 2019 Welcome to the tidyverse. *Journal of Open Source Software* **4**: 1217  
1143 1686. 1218
- 1144 Wilke, C. O., 2019 *cowplot: Streamlined Plot Theme and Plot Annotations for* 1219  
1145 *'ggplot2'*. R package version 1.0.0. 1220
- 1146 Wilkes, H. G. *et al.*, 1967 Teosinte: The closest relative of maize. Teosinte: 1221  
1147 the closest relative of maize. . 1222
- 1148 Williamson, R. J., E. B. Josephs, A. E. Platts, K. M. Hazzouri, A. Haudry, 1223  
1149 *et al.*, 2014 Evidence for widespread positive and negative selection 1224  
1150 in coding and conserved noncoding regions of *capsella grandiflora*. 1225  
1151 *PLoS genetics* **10**: e1004622. 1226
- 1152 Wright, S. I., I. V. Bi, S. G. Schroeder, M. Yamasaki, J. F. Doebley, *et al.*, 1227  
1153 2005 The effects of artificial selection on the maize genome. *Science* 1228  
1154 **308**: 1310–1314. 1229
- 1155 Xue, A. T., D. R. Schrider, and A. D. Kern, 2021 Discovery of ongoing 1230  
1156 selective sweeps within *anopheles* mosquito populations using deep 1231  
1157 learning. *Molecular biology and evolution* **38**: 1168–1183. 1232



1158 **Supplement I**  
1159 **Population sampling locations**

**Table S1 Population sampling location information.**

Population	Subspecies	Sample size	Latitude	Longitude	Elevation (meters)	Accession ID
Crucero Lagunitas	Maize	10	16.98	-99.28	201	2373-GRO-294
Amatlán de Cañas	Maize	10	20.82	-104.41	760	5054-NAY-310
Los Guajes	Maize	10	19.23	-100.49	985	TC-300
San Lorenzo	Maize	10	19.94	-103.99	982	RMM-15
Palmar Chico	Maize	55	18.64	-100.35	1008	JSG-RMM-LCL-529
Crucero Lagunitas	Teosinte	10	16.85	-99.06	590	JSG-RMM-LCL-487
Amatlán de Cañas	Teosinte	10	20.82	-104.41	880	JSG-JRP-ERG-543
El Rodeo	Teosinte	10	16.35	-97.02	982	JSG-RMM-LCL-486
Los Guajes	Teosinte	10	19.23	-100.49	851	JSG Y RMM-454
San Lorenzo	Teosinte	10	19.94	-103.99	982	RMM-13
Palmar Chico	Teosinte	50	18.64	-100.35	983	JSG-RMM-LCL-528



1160 **Supplement II**  
 1161 **Further assessment of f4 statistic inferences**

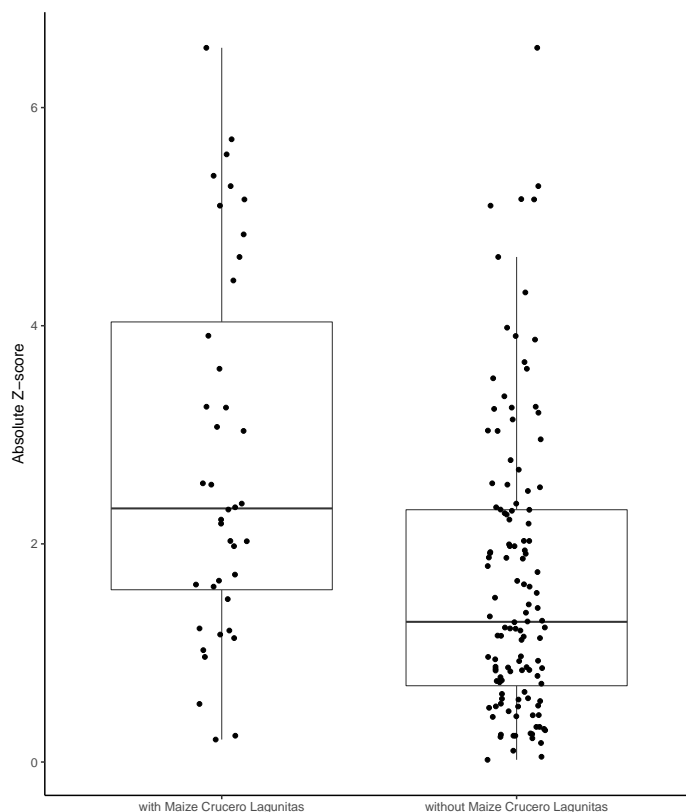


**Figure S1** f4 tests including the maize Crucero Lagunitas population are significantly elevated compared to those without.

**Table S2** Significant F4 tests. Each row of the table reports the number of significant f4 tests that occurred with a given focal and secondary population, where the two other tip positions were filled with each of the remaining populations for each subspecies. Rows that are left blank in the secondary column are used to report the total number of significant trees for a given focal population.

Focal population	Secondary population	Count
Maize Amatlan de Canas		5
Maize Amatlan de Canas	Maize Crucero Lagunitas	5
Maize Amatlan de Canas	Teosinte Amatlan de Canas	3
Maize Amatlan de Canas	Teosinte El Rodeo	2
Maize Amatlan de Canas	Teosinte Palmar Chico	2
Maize Amatlan de Canas	Teosinte San Lorenzo	2
Maize Amatlan de Canas	Teosinte Los Guajes	1
Maize Crucero Lagunitas		15
Maize Crucero Lagunitas	Teosinte Amatlan de Canas	9
Maize Crucero Lagunitas	Teosinte Crucero Lagunitas	6
Maize Crucero Lagunitas	Teosinte El Rodeo	6
Maize Crucero Lagunitas	Maize Palmar Chico	5
Maize Crucero Lagunitas	Maize Los Guajes	4
Maize Crucero Lagunitas	Teosinte San Lorenzo	4



Maize Crucero Lagunitas	Maize Amatlan de Canas	3
Maize Crucero Lagunitas	Maize San Lorenzo	3
Maize Crucero Lagunitas	Teosinte Palmar Chico	3
Maize Crucero Lagunitas	Teosinte Los Guajes	2
<hr/>		
Maize Los Guajes		6
Maize Los Guajes	Teosinte Amatlan de Canas	4
Maize Los Guajes	Maize Crucero Lagunitas	3
Maize Los Guajes	Teosinte Crucero Lagunitas	3
Maize Los Guajes	Maize San Lorenzo	2
Maize Los Guajes	Teosinte Palmar Chico	2
Maize Los Guajes	Maize Palmar Chico	1
Maize Los Guajes	Teosinte El Rodeo	1
Maize Los Guajes	Teosinte Los Guajes	1
Maize Los Guajes	Teosinte San Lorenzo	1
<hr/>		
Maize Palmar Chico		9
Maize Palmar Chico	Teosinte Amatlan de Canas	7
Maize Palmar Chico	Maize Crucero Lagunitas	5
Maize Palmar Chico	Teosinte Palmar Chico	4
Maize Palmar Chico	Teosinte El Rodeo	3
Maize Palmar Chico	Maize Los Guajes	2
Maize Palmar Chico	Maize San Lorenzo	2
Maize Palmar Chico	Teosinte San Lorenzo	2
Maize Palmar Chico	Teosinte Crucero Lagunitas	1
Maize Palmar Chico	Teosinte Los Guajes	1
<hr/>		
Maize San Lorenzo		6
Maize San Lorenzo	Teosinte Amatlan de Canas	4
Maize San Lorenzo	Maize Crucero Lagunitas	3
Maize San Lorenzo	Maize Los Guajes	2
Maize San Lorenzo	Teosinte Crucero Lagunitas	2
Maize San Lorenzo	Teosinte El Rodeo	2
Maize San Lorenzo	Teosinte Palmar Chico	2
Maize San Lorenzo	Maize Palmar Chico	1
Maize San Lorenzo	Teosinte Los Guajes	1
Maize San Lorenzo	Teosinte San Lorenzo	1
<hr/>		
Teosinte Amatlan de Canas		11
Teosinte Amatlan de Canas	Maize Crucero Lagunitas	9
Teosinte Amatlan de Canas	Maize Palmar Chico	4
Teosinte Amatlan de Canas	Maize Amatlan de Canas	3
Teosinte Amatlan de Canas	Maize Los Guajes	3
Teosinte Amatlan de Canas	Maize San Lorenzo	3
Teosinte Amatlan de Canas	Teosinte Los Guajes	3
Teosinte Amatlan de Canas	Teosinte Palmar Chico	3
Teosinte Amatlan de Canas	Teosinte San Lorenzo	3
Teosinte Amatlan de Canas	Teosinte Crucero Lagunitas	1
Teosinte Amatlan de Canas	Teosinte El Rodeo	1
<hr/>		
Teosinte Crucero Lagunitas		9
Teosinte Crucero Lagunitas	Maize Crucero Lagunitas	6
Teosinte Crucero Lagunitas	Maize Los Guajes	5
Teosinte Crucero Lagunitas	Teosinte Amatlan de Canas	4
Teosinte Crucero Lagunitas	Teosinte El Rodeo	4
Teosinte Crucero Lagunitas	Maize Palmar Chico	3



Teosinte Crucero Lagunitas	Maize San Lorenzo	3
Teosinte Crucero Lagunitas	Maize Amatlan de Canas	1
Teosinte Crucero Lagunitas	Teosinte Palmar Chico	1
Teosinte Los Guajes	Maize Crucero Lagunitas	3
Teosinte Los Guajes	Teosinte Amatlan de Canas	3
Teosinte Los Guajes		3
Teosinte Los Guajes	Maize Los Guajes	1
Teosinte Los Guajes	Maize Palmar Chico	1
Teosinte Los Guajes	Maize San Lorenzo	1
Teosinte Palmar Chico		8
Teosinte Palmar Chico	Maize Crucero Lagunitas	5
Teosinte Palmar Chico	Teosinte Amatlan de Canas	5
Teosinte Palmar Chico	Maize Palmar Chico	4
Teosinte Palmar Chico	Maize Los Guajes	3
Teosinte Palmar Chico	Maize San Lorenzo	3
Teosinte Palmar Chico	Teosinte El Rodeo	2
Teosinte Palmar Chico	Maize Amatlan de Canas	1
Teosinte Palmar Chico	Teosinte Crucero Lagunitas	1
Teosinte San Lorenzo	Maize Crucero Lagunitas	5
Teosinte San Lorenzo		5
Teosinte San Lorenzo	Teosinte Amatlan de Canas	3
Teosinte San Lorenzo	Maize Palmar Chico	2
Teosinte San Lorenzo	Teosinte El Rodeo	2
Teosinte San Lorenzo	Maize Amatlan de Canas	1
Teosinte San Lorenzo	Maize Los Guajes	1
Teosinte San Lorenzo	Maize San Lorenzo	1



1163 **Supplement III**

1164 **Predicting  $\alpha$  by mutation type**

1165 Estimates of  $\alpha$  may be effected by differences in the mutation rates of different nucleotides and genomic regions. GC biased gene conversion has been  
 1166 shown to reduce  $\alpha$  by making it harder to purge slightly deleterious alleles [Hämälä and Tiffin \(2020\)](#). Likewise, the higher mutation rates observed at  
 1167 methylated cytosine bases increases the rate of  $C \rightarrow T$  mutations [Ossowski et al. \(2010\)](#), which is another mechanism that could result in variation in  $\alpha$   
 1168 by changing the ability to purging deleterious alleles, or by changing the probability of fixation of new adaptive mutations.

1169 To study this, we used the same approach as [Hämälä and Tiffin \(2020\)](#), where we separated the site frequency spectra based on mutation types  
 1170 according to whether the ancestral and derived nucleotides had a single (weak) or double (strong) hydrogen bond between the DNA strands. As such,  
 1171 we studied three mutations types:  $A/T \rightarrow G/C$  mutations (WS),  $G/C \rightarrow A/T$  (SW) and  $C/G \rightarrow G/C$  or  $A/T \rightarrow T/A$  (SS\_WW).

1172 Unlike patterns found in *Arabidopsis* ([Hämälä and Tiffin 2020](#)),  $\alpha$  was highest for WS mutations, although there was considerable overlap between  
 1173 the credible intervals for all mutation types.

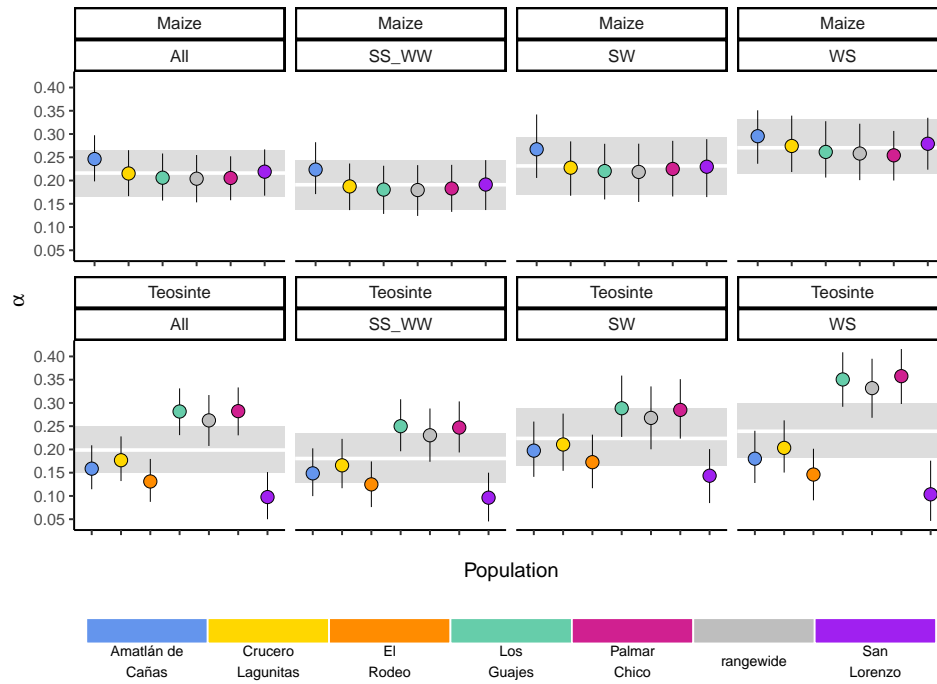


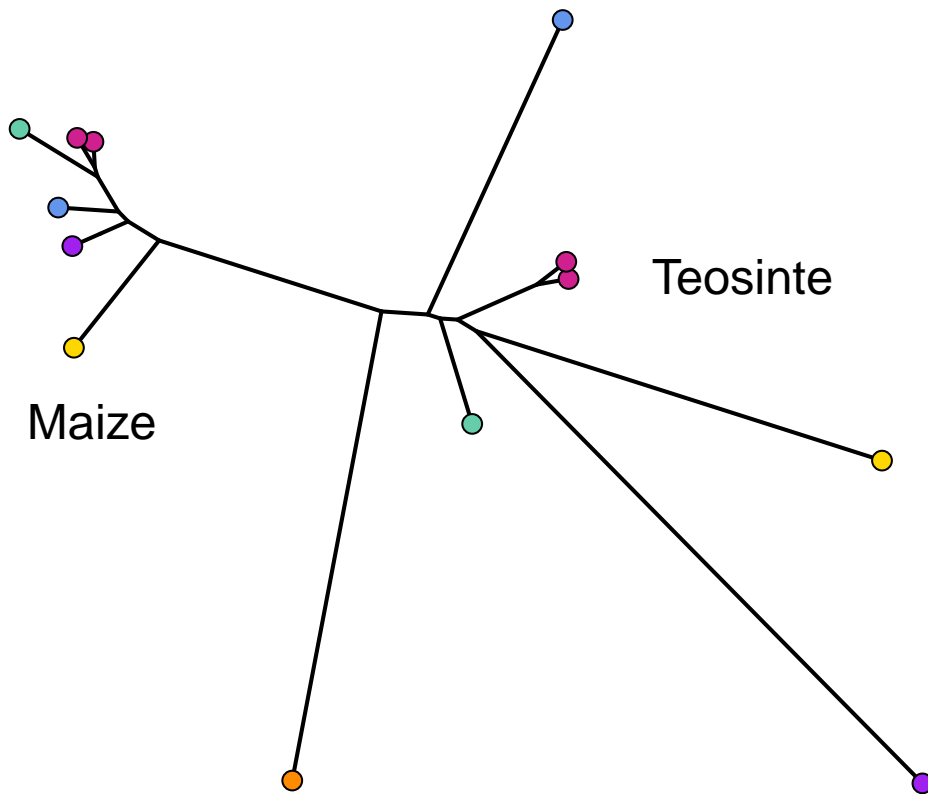
**Figure S2** Predicted values of  $\alpha$  across mutation types. Grey bands for each mutation type show the 95% credible intervals averaged over each population.



1174 **Supplement IV**  
1175 **Further assessment of sweep inferences and precision**

1176 We found that only 67% and 80% of sweeps were shared between the two random subsamples for maize and teosinte populations from Palmar Chico,  
1177 respectively (see Results). While our updated method to identifying sweeps improved precision over our previous one (which shared 40% and 50%  
1178 (Tittes *et al.* 2021)), the low precision still warrants further exploration.

1179 One explanation for the low sweep precision could be substructure within the Palmar Chico populations, leading to replicates with slightly different  
1180 histories. This could create unequal power to detect sweeps if, for example, the subpopulations had different progress towards fixation of the beneficial  
1181 allele. However, this explanation is unlikely as individuals were randomly assigned to subpopulations, so any substructure is likely to be distributed  
1182 evenly between the two samples. This is further supported from the two samples showing relatively short branch lengths in the population phylogeny  
1183 (Figure S3). The branch lengths separating the two subsamples (cophenetic distance) was 0.00835 and 0.00962 for maize and teosinte respectively,  
1184 compared to the within subspecies means of 0.0170 and 0.0559.



1185 **Figure S3 Treemix phylogeny including both subsamples of Palmar Chico.**

1186 Another potential explanation for lowered sweep sharing between replicates is that sweeps vary in their detectability based on their characteristics.  
1187 Namely, sweeps that were weakly selected, incomplete, and/or ones that started at a high initial frequency prior to the onset of selection (soft sweeps)  
1188 may vary in their detectability using the methods we employed. We conducted a simulation experiment to better understand the potential causes of the  
1189 low shared proportion, and to measure performance to detect different kinds of sweeps more generally. We used discoal (Kern and Schrider 2016) to  
1190 simulate sweeps in a 400Kb region using the average genome-wide maize mutation and recombination rates under the inferred demographic history  
1191 of the maize population from Palmar Chico (Figure 2). We simulated four distinct scenarios: classical hard sweeps, where selection acts to fix an an  
1192 adaptive mutation; soft sweeps, where selection is initiated after the adaptive allele reaches a specified frequency; and incomplete sweeps, where a hard  
1193 sweep simulation is stopped at a specified frequency, and neutral simulations without selection. For soft sweeps, we varied the initial by drawing from  
1194 a beta distribution with shape parameters 1 and 20. Incomplete sweeps finished when the adaptive allele reached a frequency of 0.5. For all three types  
1195 of sweeps, we also varied the strength of selection using the parameter  $\alpha = 4N_0s$  to be 10, 50, or 100, where  $N_0$  is the present day effective population  
1196 size and  $s$  is the selection coefficient. In addition to matching demography and other parameters, we used the same sampling scheme, simulation 50  
1197 individuals, than randomly choosing two non-overlapping subsets of 10 individuals ([https://github.com/silastittes/ms\\_sub](https://github.com/silastittes/ms_sub)). From the simulations we  
1198 assessed the True/False Positive/Negative Rates for each combination of sweep type and strength of selection ( $\alpha$ ), as well as the distribution of base  
1199 pair overlap between sweep regions inferred in the the two random subsamples. The same sweep inference methods and parameters were used for  
1200 these simulations and the empirical samples (see methods). Overall, we found that sweep characteristics we explore indeed impacted our overall  
1201 power to detect them, and the about of overlap between the sweep regions. Namely, weakly selected sweeps had consistently lower True Positive Rates  
(Table S3).



**Table S3 Performance to detect simulated hard, soft, and incomplete sweeps under varying strengths of selection under the maize Palmar Chico population demography. TPR, TNR, FNR, and FPR stand for true positive, true negative, false negative, and false positive rates, respectively.**

$4N_e s$	simulation type	TPR	TNR	FNR	FPR
10	hard	0.14	0.67	0.86	0.33
50	hard	0.92	0.75	0.08	0.25
100	hard	0.99	0.84	0.01	0.16
10	incomplete	0.04	0.67	0.96	0.33
50	incomplete	0.06	0.67	0.94	0.33
100	incomplete	0.05	0.63	0.95	0.37
10	soft	0.13	0.71	0.87	0.29
50	soft	0.75	0.74	0.25	0.26
100	soft	0.81	0.76	0.19	0.24

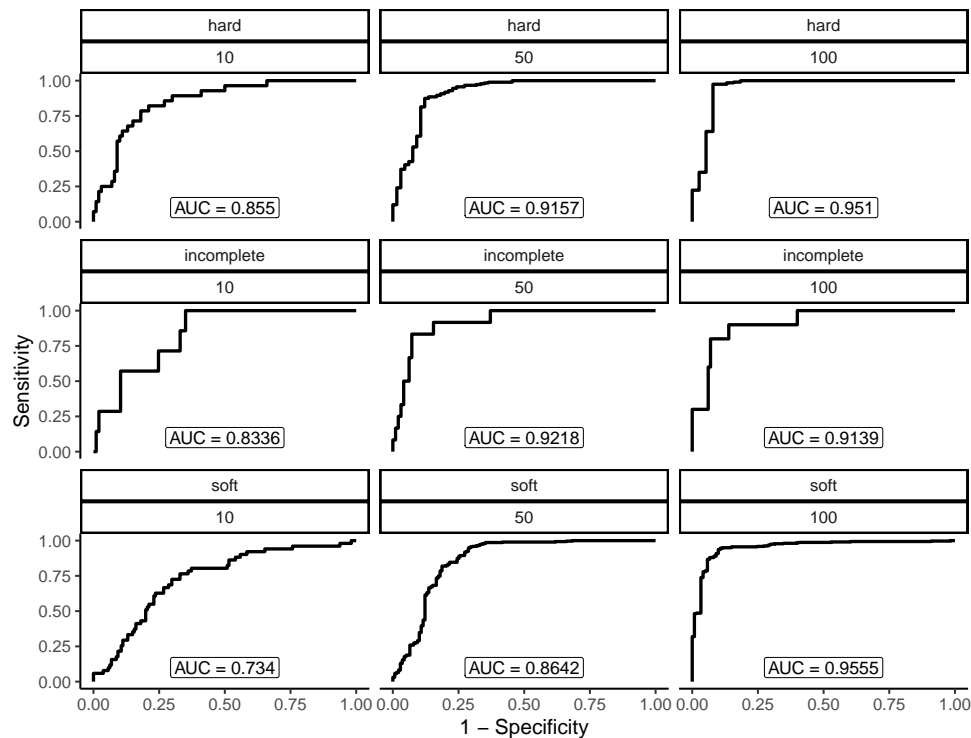


**Figure S4 Performance to detect simulated hard, soft, and incomplete sweeps under varying strengths of selection under the maize Palmar Chico population demography.** Each panel shows a combinations of sweep type (hard, soft, or incomplete) and strength of selection ( $\alpha = 4N_e s = 10, 50, \text{ or } 100$ )



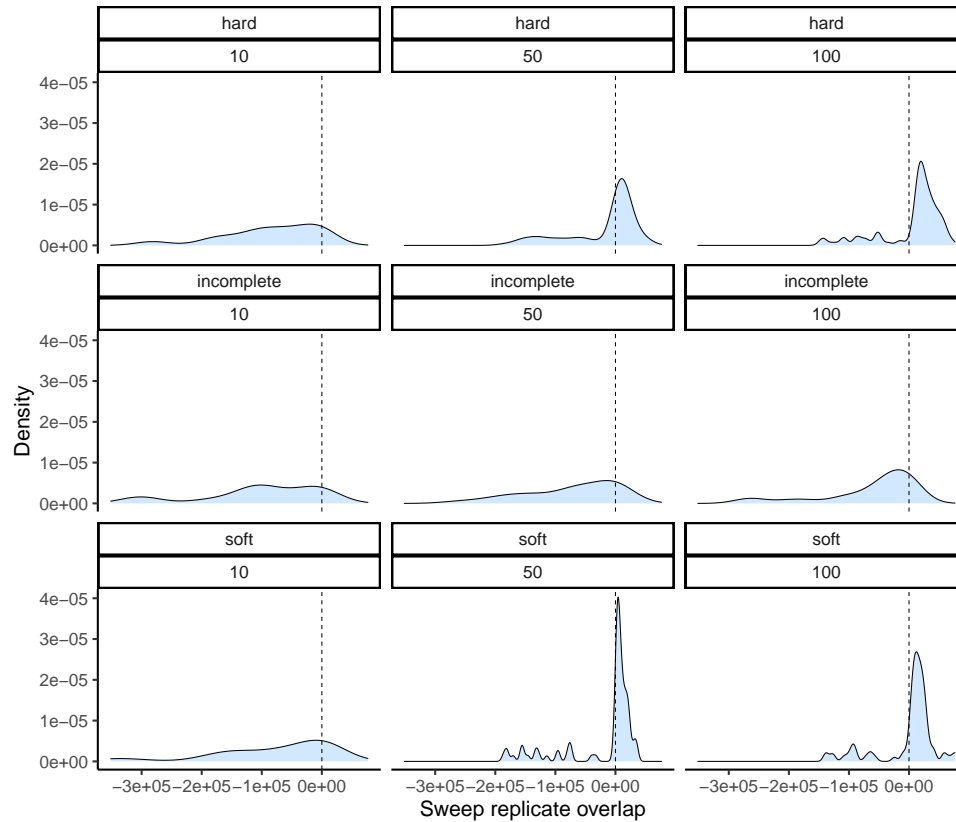


**Figure S5 Degree of overlap between simulated sweep regions taken from two downsampled replicates under the maize Palmar Chico population demography.** Positive values show the amount of overlap in basepairs between sweep regions, while negative values represent the space between them. Panel structure follows that of [S4](#).

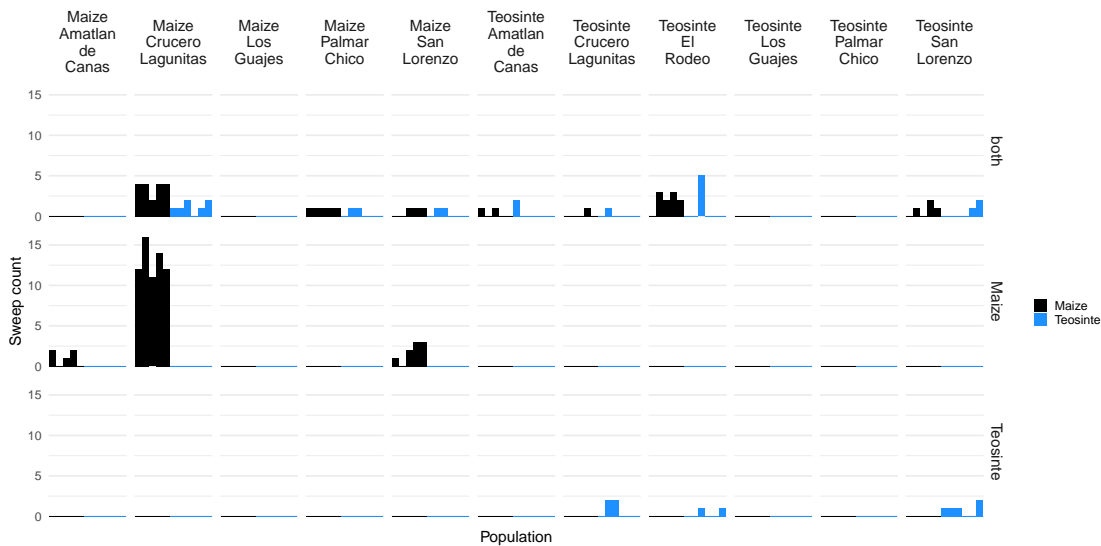


**Figure S6 Frequency of each population as the mutation source for sweeps shared via migration.** The order of populations along the x axis matches that of the source populations labeled for each strip along the top.



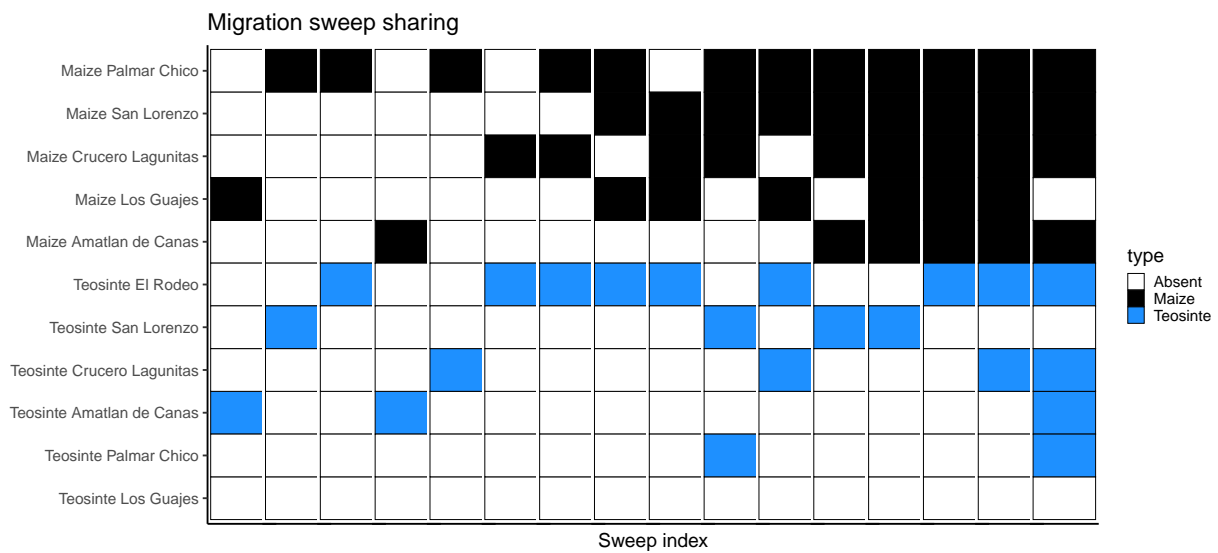


**Figure S7 Inferred sweeps shared between subspecies via migration.** The x axis is sorted by the number of populations each sweep was found in. Populations are sorted along the y axis first by subspecies then by their number of sweeps.

